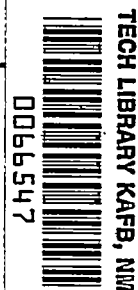


NACA TN 3495 8776



NATIONAL ADVISORY COMMITTEE FOR AERONAUTICS

TECHNICAL NOTE 3495

FAILURE OF MATERIALS UNDER COMBINED REPEATED STRESSES
WITH SUPERIMPOSED STATIC STRESSES

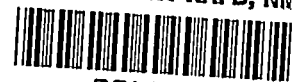
By George Sines

University of California at Los Angeles



Washington
November 1955

AFM 76
TECHNICAL
AFL 290



TECHNICAL NOTE 3495

FAILURE OF MATERIALS UNDER COMBINED REPEATED STRESSES
WITH SUPERIMPOSED STATIC STRESSES

By George Sines

SUMMARY

A review of experiments on biaxial alternating stresses and simple combinations of static stress with alternating stress is shown to lead to a general criterion for the effect of static stress on the permissible amplitude of alternating stress. The proposed criterion is then shown to agree with results from tests that have been performed under more complex stress states. Tests were performed to determine the effect of static compression on alternating torsion, the one simple combination that had not been previously investigated. These results also agree with the criterion. It is shown that Orowan's theory of fatigue can be modified to predict the observed effect of mean stress on the permissible amplitude of alternating stress.

INTRODUCTION

Many machine parts and structures must withstand combinations of alternating and static stresses. A precise knowledge of the manner in which alternating and static stresses combine to cause failure is necessary to permit design for the desired strength without using excessive material, because it is often necessary to minimize the inertial forces of moving parts, the weight of parts to be lifted, the size, or the cost. The existing criteria do not take full advantage of the strength of the materials. These criteria are discussed after the experimental results are presented in order that they may be compared. Not only is an accurate design criterion essential, but the nature of the mechanism within the material that leads to fatigue failure may be revealed if the variables are isolated and the functional relations between them are established. Therefore, experimental evidence is analyzed for the purpose of obtaining a design criterion and insight into the mechanism of the fatigue failure.

It is necessary for experimental investigators to simplify the fluctuating stress in such a way that parameters can be identified and their influence on the behavior observed. A brief examination of the general fluctuating stress state will illustrate its complexity and reveal the

extent of the simplification. A stress can be described by three principal components and their directions as arbitrary functions of time, but such a general time description is not amenable to identification of parameters. However, if only periodic functions of simple shapes are considered, the description is simplified to an alternating stress superimposed upon a static stress, thus reducing the description to:

- (1) Three numbers to designate the principal components of the static stress
- (2) Three numbers to give the amplitudes of the alternating principal stress components
- (3) Two numbers to give phase relations between the alternating stress components
- (4) Three numbers to give the space orientation between the static and alternating stress components
- (5) The three frequencies of the alternating stress components
- (6) A description of the shape of the periodic function

The stress states considered in this investigation are limited to:

- (1) Biaxial or uniaxial static stress
- (2) Biaxial or uniaxial alternating stress
- (3) Alternating stress components that are either inphase or out-of-phase (two components are out-of-phase if one of them reaches its maximum tension at the time when the other reaches its maximum compression)
- (4) A space orientation between the static and alternating stress components that is independent of time
- (5) The same frequencies for both of the alternating components (which are in a range where the effect of the frequency is negligible)
- (6) Periodic functions of approximately sinusoidal shape

Considering the effects of the biaxial instead of the triaxial state of stress is not such an oversimplification as it may at first seem to be. Most fatigue cracks, in fact, begin at the surface of machine parts where a biaxial state of stress exists. These cracks are initiated at the surface instead of in the interior of the part because

(1) Many parts are stressed by bending and torsion in which the highest stresses occur at the surface.

(2) Surface stress may be increased by the presence of "stress concentrations," for example, scratches, roughness, and notches.

(3) Some investigators of fatigue believe that the crystalline grains that form the surface of a metal are inherently weaker under stress because their deformation is not confined by the presence of adjoining grains on the one side.¹

Experiments in which the stresses have been restricted in the above manner are examined to see how the alternating stresses combine to cause fatigue failure and how the permissible range of alternating stress is affected by the static stresses. Knowledge of the effects of even simple stress systems is useful for design and may possibly be extended to more complex systems or may reveal something of the mechanism of the fatigue phenomenon.

Experiments on the behavior of materials subjected to various combinations of alternating biaxial stresses are considered first. After the effects of the alternating stresses have been established, experiments are examined to see the effect of the static stresses superimposed upon the alternating stresses. Experiments by Gough (ref. 1), in which various combinations of alternating torsion and bending were used, are examined, for they are extensive and agree with those of other investigators (refs. 2 and 3). The principal stresses from combined bending and torsion are always out-of-phase; that is, one stress reaches its greatest tensile value as the stress orthogonal to it reaches its greatest compressive value. Sawert's tests (ref. 4) are the only ones known to the author in which various combinations of alternating inphase stresses have been obtained. The ratio of the pure torsional fatigue strength to the pure bending fatigue strength is also indicative of the mechanism of failure and the ratios obtained by Gough for 14 materials are examined.

¹Unpublished test results of the Douglas Aircraft Company show that the fatigue strength of axially stressed specimens is improved about 25 percent by shot peening. It should be noted that the stress under axial loading is the same at the interior as at the surface and that peening affects only the surface. If the unpeened surface and the interior had equal strength, the shot peening would have no beneficial effect because the failure would occur in the interior at the same stress at which failure starts on the untreated surface. However, the peening did improve the fatigue strength of the axial specimens; therefore, the surface must be weaker in fatigue than the interior by at least the amount of the improvement.

Next, the results of various simple combinations of static stresses and alternating stress are examined to see in what manner static stresses influence the permissible alternation of stress for a given cyclic life.

A stress criterion for failure is proposed and compared with the experimental results for the combined alternating stress and simple combinations of alternating and static stress. This criterion is then compared with results from tests using more complex combinations of stress that have been performed by Gough (ref. 1), Roß and Eichinger (ref. 5), and Maier (ref. 6).

The research described in this report was conducted in the Department of Engineering, University of California, Los Angeles, under the sponsorship and with the financial assistance of the National Advisory Committee for Aeronautics.

The author wishes to acknowledge the many contributions to the development of the analyses made by Professor D. Rosenthal of the Department of Engineering, University of California, Los Angeles. Professor D. T. Griggs of the University of California, Los Angeles, Department of Geophysics and Professor P. W. Bridgman of Harvard University, drawing from their high-pressure studies, have made helpful suggestions on the effect of static stress on fatigue.

SYMBOLS

b	reversed bending fatigue strength
f	amplitude of alternating normal stress caused by bending
N_1, N_2	static normal stresses on planes of maximum alternation of shear
P_1, P_2, P_3	principal static stresses, ordered $P_1 > P_2 > P_3$
p_1, p_2, p_3	amplitudes of alternating principal stresses, ordered $p_1 > p_2 > p_3$
q	amplitude of alternating shear stress caused by torsion
S_x, S_y, S_z	static orthogonal normal stresses
t	shear fatigue strength determined by reversed torsion test
$\sigma_1, \sigma_2, \sigma_3$	alternating orthogonal normal stresses, which are the principal stresses when ordered

τ shear stress

Subscripts:

crit critical

m mean

max maximum

min minimum

oct octahedral

A CRITERION FOR FAILURE UNDER COMBINED ALTERNATING
AND SUPERIMPOSED STATIC STRESS

Experiments With Combined Alternating Stresses

Gough's tests on combined bending and torsion.- Gough (ref. 1) has investigated experimentally the interaction of alternating bending and torsional stresses on fatigue life. A typical interaction curve for a chrome-vanadium steel is shown in figure 1(a). These data agree closely with the empirical expression that he proposed:

$$\frac{f^2}{b^2} + \frac{q^2}{t^2} = 1$$

where

f amplitude of alternation in bending stress

q amplitude of alternation of shearing stress caused by
torsion

b fatigue limit under reversed bending stress

t fatigue limit under reversed torsion

The interaction curves for cast iron have a different characteristic shape; a typical example is presented in figure 1(b).

Sawert's combined-stress tests.- The experimental difficulties involved in applying biaxial reversed stresses in different combinations in fatigue tests were overcome by Sawert (ref. 4). He applied an

alternating normal stress to a series of differently shaped specimens, each shape calculated to develop a certain desired biaxiality of stress. His results for an annealed low-carbon steel are shown in figure 2.

The coordinates are the alternating longitudinal stress and the alternating transverse stress made nondimensional by division by the uniaxial fatigue strength. The plot for tests on chrome-vanadium steel appears very much like that for the low-carbon steel.

Gough's tests on bending and on torsion.- Another indication of the stress criterion can be determined from the ratio of reversed torsional fatigue strength to reversed bending fatigue strength. Gough's data, taken from page 37 of reference 1, are listed below for several materials:

Material	$\frac{\text{Max. shear stress in torsion test}}{\text{Max. shear stress in bending test}}$
0.1-percent-carbon steel (normalized)	1.13
0.4-percent-carbon steel (normalized)	1.25
0.4-percent-carbon steel (spheroidized)	1.135
0.9-percent-carbon steel (pearlitic)	1.37
3-percent-nickel steel	1.20
$3\frac{1}{2}$ -percent-nickel steel	1.20
Chrome-vanadium steel	1.20
$3\frac{1}{2}$ -percent-nickel-chromium steel (normal impact)	1.305
$3\frac{1}{2}$ -percent nickel-chromium steel (low impact)	1.27
Nickel-chromium-molybdenum steel (60/70 ton)	1.08/1.17
Nickel-chromium-molybdenum steel (75/80 ton)	1.04
Nickel-chromium steel (95/105 ton)	1.175
"Silal" cast iron	1.82
"Microsilal" cast iron	1.67

Comparison of Behavior Under Alternating Stresses

With Static-Failure Criteria

Gough and Sawert used different coordinates to plot their test data for the effect of different combinations of alternating stress. The data should be presented in the same manner in order that the relation between the two sets of data can be seen. The presentation that has been used for failure from combined static stresses will be examined for the purpose of selecting common coordinates. Some relations that have been proposed for predicting the failure of materials from a single application of load will be examined to see whether they have any agreement with the test results obtained from repeated applications.

As mentioned previously, any stress state can be described by the three principal stresses P_1 , P_2 , and P_3 . The criteria for failure can be expressed as functions of the principal stresses. When the value of the function exceeds a certain critical value, failure is predicted; conversely, if the value remains less than the critical one, no failure is to be expected.

Mathematically expressed, if $F(P_1, P_2, P_3) \geq F_{crit}$, then failure occurs.

To see what criterion of failure is most nearly satisfied, it will be convenient to have the data plotted as functions of the normal stresses. Sawert's data, as plotted by him, are in this form, but the interaction curves of Gough will have to be transformed by the following relations:

$$p_1 = \frac{f}{2} + \sqrt{\frac{f^2}{4} + q^2}$$

$$p_3 = \frac{f}{2} - \sqrt{\frac{f^2}{4} + q^2}$$

(at the surface $p_2 = 0$), where f is the tensile stress caused by the bending moment and q is the shear stress caused by the twisting moment. The transformed data are plotted in figure 3. Point 1 is for the fatigue strength under pure alternating bending; point 2 is for pure alternating torsion. The range of biaxiality that can be obtained by combined bending and twisting is limited to the lower quadrant. The mean stress for these tests was zero; thus the tensile stress changes to compressive and the transverse compressive stress, to tensile on the reverse part of the cycle.

Several criteria for the failure of polycrystalline solids from static loads may now be examined to see what correlation exists between these criteria and the fatigue-test data of Sawert and Gough presented in figures 2 and 3.

The properties of materials and the conditions under which they are tested may differ greatly, and, also, failure may be considered to occur when there is either excessive plastic deformation or rupture. These factors cause the results of a particular static test to agree more closely with one criterion than with the others; therefore, several criteria have proved to be useful in the static case. The criteria are presented as functions of normal stresses which become the principal stresses P_1 , P_2 , and P_3 when properly ordered ($P_1 > P_2 > P_3$). Since the surface of the specimen is the region considered, the principal stress normal to the free surface is always zero.

The three most significant stress criteria for failure from static stresses may be simply described as follows:

(1) Failure may be predicted according to the maximum-normal-stress criterion whenever the principal stress exceeds a critical value. If $P_1 > \sigma_{crit}$, then failure will occur.

(2) Failure may be predicted according to the maximum-shear-stress criterion when the stress on any plane exceeds a critical value. The theory of elasticity shows that the maximum shear stress is equal to one-half the greatest difference between the principal stresses, so the criterion can be expressed as follows: If $\frac{P_1 - P_3}{2} > \tau_{crit}$, then failure will occur.

(3) Failure may be predicted according to the octahedral-shear-stress criterion if the following function exceeds a critical value, that is, if

$$\frac{1}{3} \sqrt{(P_1 - P_2)^2 + (P_2 - P_3)^2 + (P_1 - P_3)^2} > \tau_{oct-crit}$$

One interpretation of the physical significance of the octahedral-shear-stress criterion is that it expresses the average of the effects of slippage on different planes and in different directions of all crystals in the aggregate, with the slip on any given plane being caused by resolved shear stress on that plane (ref. 7). The constraint of adjoining crystals upon each other is also considered but is a factor of secondary importance. Postulating that the potential energy due to elastic distortion must not exceed a constant value is mathematically equivalent to expressing the octahedral-shear-stress criterion (ref. 8).

Other criteria of failure have been discussed by Gough (ref. 1).

The criteria are superimposed on the test data in figures 2 and 3 so that the correspondence with experimental results can be examined. In the upper quadrant all three of the criteria agree fairly well with the data. In the lower quadrant the data for steel are near the criteria for maximum shear stress and octahedral shear stress, but they deviate sharply from the criterion for normal stress. There are, however, two difficulties with the data presented. As is usual in fatigue testing, it is impractical to break enough specimens to obtain a good statistical average, and the extent of "size effect" in Sawert's work is not known, since his specimens (because of the combined stresses he sought) were necessarily of various sizes and shapes. "Size effect" describes the behavior in which material in a large part appears to have a lower fatigue strength than that in a smaller one (ref. 9). The data for steel agree fairly well with both the maximum-shear and octahedral-shear criteria, but the unavoidable scatter prevents determining which of these is better satisfied. On the other hand, Gough's tests on cast iron come nearer to the criterion for normal stress than to either of the criteria for shear stress; this behavior is discussed below in detail.

Another indication of the stress criterion can be seen by examining the ratio of the reversed torsional fatigue strength to the reversed bending fatigue strength for Gough's tests presented in the section "Experiments With Combined Alternating Stresses." The points representing the two stress states on the principal-stress diagram (fig. 3) are:

- (1) Pure bending stress, located on the abscissa
- (2) Pure torsional stress, located on the line passing through the origin and bisecting the lower quadrant

The ratios for the criteria discussed above, as well as for several additional ones, are:

Criterion of failure	<u>Max. shear stress in torsion test</u> Max. shear stress in bending test
Constant maximum shear stress	1.0
Constant maximum octahedral shear	1.15
Constant total strain energy	1.25
Constant maximum principal strain	1.56
Constant maximum principal stress	2.0

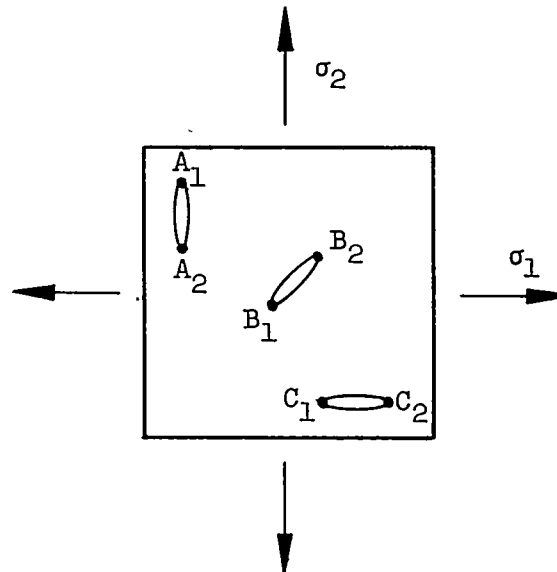
Considering the normal scatter of fatigue data, only the first two figures of the ratios can be considered really significant; these ratios are plotted in the bar diagram of figure 4, in frequency of occurrence, in 0.1 divisions. The greatest frequency of failure, consisting of the ratios for six pairs of tests, is shown to occur between 1.1 and 1.2, which indicates that the data from these particular tests in the lower quadrant most nearly satisfy the octahedral-shear criterion.

The scanty existing data do not give grounds for distinguishing whether the maximum-shear-stress criterion or the octahedral-shear-stress criterion best fits the experimental results. Moreover, the constants can be chosen so that the two criteria do not differ by more than ± 8 percent. Both sets of data indicate that alternating shear stress causes the fatigue damage, the difference being caused only by the degree of averaging and by mutual constraint of the crystals. On the basis of present experimental knowledge, then, either criterion can be justifiably applied; the only evident choice between them is the convenience of the mathematical expression in any given case.

The interaction curves for fatigue failure induced by combined torsional and bending stresses for cast iron in figures 1(b) and 3 and the ratios of torsional to bending fatigue strength in figure 4 are very close to what would be expected if the maximum principal stress were the cause of failure; however, the interaction curves for the other metals investigated lie in the region near the curves for a criterion of maximum shear stress and that of octahedral shear stress. If this difference in behavior indicates that in cast iron a completely different mechanism of fatigue failure is operative from that found in other metals, the fundamental metallurgical problem will be severely complicated. A close examination will be made in an attempt to resolve the two apparently different behaviors.

Microscopic observation of cast iron reveals many flakes of graphite dispersed throughout the metal. Graphite has a modulus of elasticity much lower than that of the surrounding iron crystals. Therefore, the flakes of graphite carry very little stress in compression, and because of their low strength they carry even less in tension. They act, in fact, like holes in the iron structure. The effect of these flakes can

be seen by considering a simplified model of three holes oriented at different angles as shown below:



Sketch 1

When σ_1 is applied, regions A_1 and A_2 at the edge of one flake will be much more highly stressed than any other region because of the elastic stress concentration caused by the hole. Regions B_1 and B_2 will also be more highly stressed than the average but still considerably less than A_1 and A_2 . Regions C_1 and C_2 around the edge of the flake longitudinal to the applied stress will be stressed even less than the average for the bulk of the material. The regions most highly stressed by the transverse stress σ_2 are C_1 and C_2 , while regions A_1 and A_2 are stressed very little. The elastic analysis of cracks oriented at different angles under several combinations of stress is presented in appendix A. The analysis shows that the sum of the effects caused by the transverse and longitudinal stresses together at cracks oriented at angles between that of A_1A_2 and C_1C_2 is less than that caused by them individually at A_1 and A_2 or C_1 and C_2 , except for the range of combinations of applied stresses where the transverse stress approaches a value equal to the longitudinal one and then the combined effect is slightly greater at one orientation than the isolated individual effects at other orientations. Thus the greatest damage from the two stresses is localized at different points, which causes their effects to be independent. The independence of the effects of the principal stresses is the essential characteristic of the behavior that indicated that the principal-stress criterion might be operative; however, the independence can be explained by the localization of the damage. Thus no evidence is given as to which of the stress criteria is applicable in the highly stressed microscopic regions; it could be a shear-stress criterion.

In all cases examined in which a maximum-normal-stress criterion best fitted the data, there has been strong reason to believe that flakes of graphite or other flakelike inclusions were present in the material. Turner's tests on annealed hypereutectoid steel (ref. 10) showed that a maximum-normal-stress criterion was more nearly satisfied than a maximum-shear-stress criterion. Graphite flakes may well have been present in the steel he used, for Sisco (ref. 11) mentioned that it was noticed many years ago that occasionally, in annealing high-carbon steel, free carbon (graphite) would form. Evidently, too, it would not take many such flake inclusions to cause the effect, for Thum and Petersen (ref. 12) studied the effect of graphitic carbon in cast iron on tensile and fatigue strength and concluded that the fatigue strength depends chiefly upon the notch effect of the particles of graphite and that this effect is great even when little graphite is present, as demonstrated by the fact that the fatigue strength decreased quite slowly as the amount of graphitic carbon was increased.

These considerations indicate, then, that, although some materials, particularly cast iron, seem to fill nearly a maximum-normal-stress criterion, the failure is not necessarily caused by normal stresses; thus it may have started from damage caused by alternation of shear stresses in the highly stressed region at the edge of a flake of graphite. Therefore, whatever theory explains the fatigue failure in the more homogeneous metals may also explain the failure of cast iron and other metals, which have previously seemed to be exceptions.

Effect of Static Stress Superimposed on Alternating Stress

From the above determination that test data and shear criteria do agree, it seems that the component of the alternating stress field that causes fatigue damage is the shear stress. To what extent the permissible amplitude of alternating stress depends upon the static stress must be examined in different stress combinations in an attempt to isolate the component or combination of components of the static stress operative in the relation. Experiments on the influence will be examined:

- (1) The effect of static tension on the permissible amplitude of alternating axial stress and the effect of static compression on the permissible amplitude of alternating axial stress (fig. 5)
- (2) The effect of static torsion on the permissible amplitude of alternating torsion (fig. 6)
- (3) The effect of static torsion on the permissible amplitude of alternating bending (fig. 7)

(4) The effect of static tension on the permissible amplitude of alternating torsion and the effect of bending on the permissible amplitude of alternating torsion (fig. 8)

Figure 5 shows the effect of mean axial stress on the permissible amplitude of alternating axial stress for some common materials with fatigue lives of 10^6 to 10^7 cycles. Quite clearly, the amplitude of alternating stress is decreased by the tensile mean stress and is increased by the compressive mean stress. The choice of coordinates was not made in order to imply a dependence of the slope on the yield strength but as a convenient way of presenting the group of separate curves and yet emphasizing the behavior in the region below the yield; moreover, Nishihara and Sakurai (ref. 13) have shown in some cases that there is a dependence of the slope on the true rupture strength.

Only by critical selection of the data for the compressive region was it possible to plot the considerable slope shown; if all investigations were included, the trend would be horizontal (ref. 14). The technical difficulties of applying a true axial compressive load are considerable, and it is likely that uncontrolled bending stresses have invalidated some tests. Those cited here were chosen because the techniques employed seem to insure true axial loading.

In Nishihara and Sakurai's tests, the load was transmitted to the specimen through an arrangement containing a ball resting on a flat surface. Thus the exact position of the force was known and it could be centered accurately on the axis of the specimen.

Newmark and coworkers (ref. 15) and Roš and Eichinger (ref. 5) used specimens with carefully squared ends in attachments that made the gripping heads remain parallel and concentric during the stress cycle. They also checked the axiality by means of electric strain gages.

The relation is linear in the region where maximum stress does not exceed the yield strength. If only fatigue rupture (not yielding) is considered to be failure, the linear part of the curve has been shown to extend beyond the yield strength and then to turn sharply to the abscissa, intersecting it at the point of static rupture strength (ref. 5).

Figure 6 shows the effect of static torsion on the permissible amplitude of alternating torsion. The great number of tests plotted gives conclusive proof that static torsion has no effect on the permissible

range of alternation so long as the maximum torsional stress is below the yield strength.²

Figures 7(a) and 7(b) show the available data on the effect of static torsion superimposed on alternating bending stresses. From the few tests plotted, it seems that bending fatigue strength is not affected until static torsion exceeds the torsional yield strength by almost 50 percent.³

Figure 8 shows the only two tests known to the author of the effect of tensile static stress on the permissible amplitude of alternating torsion. In one test the tensile stress was produced by bending, while in the other it was produced by an axial load. The linear dependence of the amplitude of alternating torsion upon the applied static tensile stress is similar to that shown in figure 5, which presents the effect of static axial stress on the amplitude of axial stress.

It was inferred from the agreement of the fatigue tests under combined alternating stresses with the shear-stress criteria that the alternation of shear stresses causes the fatigue damage and the resultant failure. The preceding presentation of the effect of different static stresses on the permissible amplitude of alternating stress was made in an attempt to isolate the effective parameters and reveal the functional relation of the static stress to the permissible amplitude of alternating stress. The behavior is summarized in figure 9.

²Plotting fatigue tests taken at only one mean stress for materials having different yield strengths could give a deceptive horizontal line because the abscissa is the ratio of the maximum shear stress to the yield strength; but examination of a series of tests on one material in which the maximum stress was varied appreciably, for example, Ludwik and Krystof's tests on Siemens-Martin steel (ref. 16) or Moore and Lewis' tests on duralumin (ref. 17), shows that the observation is a valid one, and not the result of the choice of the coordinate.

³Davies, in a discussion of the paper of Gough and Pollard (ref. 18), presented some experiments that show that static torsion does influence the alternating bending strength; these data contradict those of Lea and Budgen (ref. 19) and of Ono (ref. 20). The sources of his information were the masters theses of Nimhamminne (ref. 21) and Huitt (ref. 22) at the Battersea Polytechnic Institute. Examination of these theses reveals that their "fatigue strength" was not obtained by fracture of a series of specimens but was defined as that stress at which nonlinear deflection occurs under increasing alternating stress. This "fatigue strength" may be useful in particular designs where nonlinear deflection can be construed as failure, but it is not the conventional fatigue strength and should not be compared with that of the other investigators. Although it was not mentioned, the device used to apply the static torsional stress appears inadvertently to apply a static bending stress. This could also contribute to the observed anomalous behavior.

Because the alternation of shear stress seems to cause the fatigue failure, the static stresses on the planes of greatest alternation of shear will be examined. The planes are identified on the specimens illustrating the stress state and are shown magnified in the center column together with the static stresses that act on them (fig. 9).

A simple correlation appears between the sum of the normal static stresses on these planes and the variation of the permissible amplitude of alternating stress. For example, examination of stress state (1), the effect of tension on the amplitude of shear, shows that, when the sum $N_1 + N_2$ increases, the amplitude is decreased. When the sum is zero, as in combination (3), the effect of torsion on the amplitude of bending, the permissible amplitude of alternating stress is independent of the static stress.

The sum of the normal stresses on orthogonal planes has been shown in the theory of elasticity to be independent of the orientation of the planes to the stress field (ref. 23). (The sum is called the first invariant of the stress tensor.) Therefore, the relation can be expressed more generally as a function of the sum of any other convenient orthogonal normal stresses instead of as the sum of the normal stresses on the planes of maximum alternating shear.

A review of the data presented in figures 5, 6, 7, and 8 will show that a linear function closely approximates the effect of static stress on the permissible amplitude of alternating stress if the stresses do not exceed the yield strength. Because of the scatter inherent in fatigue tests, a higher order of approximation would not be justified. A general stress criterion may be postulated that agrees with all the above data and with the combined-alternating-stress data that were previously presented. In this expression it is convenient to use the octahedral shear stress, because it is independent of the orientation of the orthogonal stress coordinates in the same way that the sum of the orthogonal normal stresses is. The general criterion combines the shear criterion for combined alternating stress with the linear relation of the amplitude of alternating stress to the static stress. This general criterion may be expressed as

$$\frac{1}{3} \sqrt{(p_1 - p_2)^2 + (p_1 - p_3)^2 + (p_2 - p_3)^2} \leq A - \alpha(S_x + S_y + S_z)$$

where p_1 , p_2 , and p_3 are the amplitudes of the alternating principal stresses, S_x , S_y , and S_z are the orthogonal static stresses, A is a constant for the material proportional to the reversed fatigue strength, and α gives the variation of the permissible range of stress with static stress; A and α are also dependent on the number of cycles to failure.

The term on the left must not exceed that on the right or failure will occur before the desired lifetime. The amplitudes of the alternating principal stresses do not have to be ordered $p_1 > p_2 > p_3$ in the criterion because their differences are squared in it.

Two tensile fatigue tests, one with a zero mean stress and the other with a high positive mean stress (but not so high that the maximum stress exceeds the yield strength), could be conveniently used to determine the two constants.

Expressed more briefly in terms of the tensor invariants, the square root of the second stress invariant of the alternating stress is a linear function of the first invariant of the static stress

$$J_2^{1/2}_{\text{alternating}} \leq B - \beta J_1_{\text{static}}$$

where B and β differ from the previously defined A and α by a multiplicative constant.

A graphical representation of the criterion for the failure of a body at a free surface is shown in figure 10. Early paragraphs of this report give some reasons why consideration of the surface is of more interest than consideration of the interior. At a free surface one principal stress is zero; therefore the criterion can be plotted on a two-dimensional space of the other two principal stresses. The more positive the sum of the static stresses, the smaller the ellipse. The plot appears as a series of "concentric" ellipses, the size of which is dependent upon the sum of the static normal stresses. The shape of the ellipses (ratio of axes) was fixed by the insertion of the octahedral shear into the criterion.

Another axis orthogonal to the two of figure 10 is needed for the representation of the criterion when it is applied to the interior of a body. The failure surface in this space is a cylindrical surface with generators having the directional cosines $1/\sqrt{3}$, $1/\sqrt{3}$, and $1/\sqrt{3}$ intersecting the planes of the axes in the ellipses shown in the two-dimensional representation (ref. 24).

Comparison of Proposed Criterion With

Complex Combinations of Stress

Gough's tests.— Gough has performed some tests that may be used to support the general criterion (ref. 1). The tests were conducted not

only under different combinations of alternating stress but also under different combinations of static stress. Specimens of nickel-chromium-molybdenum steel were subjected to combined alternating bending and torsion superimposed on static bending and torsion. The static stress, and thus the sum of the static normal stresses, was kept constant for each of the two series of combined alternating stresses shown in figure 10; therefore, the test results should be expected to fall close to the ellipses, which are lines of constant sum of the normal stresses. The data are for failure at 10^7 cycles of stress.

Gough's empirical formula fitted the data closely on the original bending-torsion interaction curves, so it was transformed with the data to the principal stress plane. The empirical curves appear in the graph as the dotted lines. The data as well as the empirical curves are seen to lie close to the solid elliptical curves which represent the general stress criterion. Several other tests were given but not reproduced here because the effect from the smaller values of the static stress used in those cases could be obscured easily by the considerable scatter of the data.

Roš's tests.- Professor M. Roš, at the Swiss Federal Material Testing and Research Institute, Zurich, has conducted extensive tests on the fatigue strength of several materials under combined stresses that varied between no stress and the maximum stresses (ref. 5). The specimen was a hollow cylinder in which hydraulic pressure caused a hoop stress, to which was superimposed a longitudinal stress from an external force. Some typical results are plotted in figures 11(a) and 11(b). The curves are for a cyclic life of 10^6 stress cycles. Other investigators have found similar results (refs. 25 and 26).

The general criterion was presented as a function of the sum of the normal static stresses, but it can be transformed to the test variables used by Roš. The stress components in this case varied between no stress and the maximum stress; thus, the static stress components are different for each combination of the alternating stress and are equal to the amplitudes of the alternating stresses. The mathematics of the transformation is performed in appendix B. The results are plotted in figures 11(a) and 11(b) as an ellipse inclined at 45° to the axes and displaced toward the bottom left.

It is seen that the ellipse fits rather closely the test data for the cast steel and agrees fairly well with those for aluminum.

Maier's tests.- Still another experiment tends to confirm the proposed criterion. Maier (ref. 6) performed tests by applying hydraulic pressure to the interior of a cylinder with closed ends so that the longitudinal stress was equal to about one-half of the circumferential stress. Longitudinal constraint was applied in some tests to cancel the

longitudinal stress, so that only circumferential stress was present. The stress cycle was between zero stress and maximum stress (the same as Roš's), thus making the mean stress (the static stress) equal to the amplitude of the alternating stress. Maier's experiments showed that the constraint had no effect on circumferential fatigue strength.

In appendix B, the general criterion in which the permissible amplitude of octahedral shear stress is a linear function of the static stress is transformed for the stress cycle, which varies from zero to maximum. If one inserts into the transformed criterion a fairly typical value for the zero-to-compression fatigue strength, that is, a value one and one-half times as great as that for zero-to-tension fatigue strength, then it is found that the superimposition of the circumferential stress on a longitudinal stress equal to one-half the circumferential results in a predicted fatigue strength no different from that found where no longitudinal stress is applied. This can also be seen in figure 11(a) where, if a line were passed parallel to the abscissa through the point of intersection of the ellipse with the ordinate ($\sigma_1 = 0$, $\sigma_2 = 28$), it would intersect the ellipse again at $\sigma_1 = 14$, $\sigma_2 = 28$. Thus, Maier's data agree closely with the general criterion.

Maier interpreted his tests to indicate that the maximum-shear criterion for static failure applied instead of the octahedral, because the maximum-shear criterion is independent of the intermediate stress (in this case the longitudinal) and the octahedral criterion is a function of the intermediate stress. Certainly neither the simple octahedral criterion nor a simple maximum-shear criterion that contains only one set of stresses can be applied to a case where static stresses are superimposed upon the alternating ones, because the criterion must be a function of both the alternating and static stresses.

Selection of test variables for complex-stress tests.- Attention should be paid to the selection of the test parameters for fatigue tests under combined stresses, so that the results will have as great an applicability as possible for the prediction of behavior.

One choice of parameters would be to fix the ratio of minimum to maximum stress for the alternating principal stresses for each series of stress combinations. Assuming that the general stress criterion proposed does predict the behavior, its transformation to this set of parameters is calculated in the appendix for a given cyclic life and appears graphically in figure 12(a).

A series of combined-alternating-stress tests could be performed with another selection of parameters in which the static stress was maintained constant for each combination of the series and changed for each series. These tests would appear as the ellipses shown in figure 12(b).

The two methods for obtaining and presenting the information are equally good so long as both principal stresses have the same ratio of minimum to maximum stress; however, if the ratio is different, then the first plot has no utility. The usefulness of the second method is even greater because the ellipses are not only lines of constant static stress but lines of constant sum of the orthogonal static stress components. Thus, it would be more general to take data by the second method using the static stress as a parameter, holding it constant for individual alternating stress combinations and changing it from one series to the next.

Limitations of criterion.- The general criterion proposed is not useful as a design criterion for cast iron, hypereutectoid steels, or other metals that also might contain flakelike inclusions or microcracks; the impossibility of obtaining detailed information concerning the cracks and inclusions prevents the application of the general criterion. Gough and others showed that a maximum-normal-stress criterion is applicable to the aggregate (see ref. 1).

Also, the axial fatigue strength of cast iron is not a linear function of the static stress; compressive stress improves the fatigue strength more than tensile stress reduces it. The rather complicated relation was shown by Roř and Eichinger (ref. 5).

Discussion of Previously Proposed Criteria for Fatigue Failure

An attempt was made by Bailey (ref. 27) to predict the effects of combined alternating and static stresses. At that time, 1917, most of the data presented in the derivation of the general criterion had not been taken. Bailey decided from examination of Stanton and Batson's results (ref. 28) from tests under alternating bending and alternating torsion that "in the absence of evidence to the contrary, then, the most reasonable assumption to make in pursuing the object in view is that under all combinations of bending moment and twisting moment, either variable or constant in magnitude, the failure of a ductile material is by shear, uninfluenced by the presence of normal stress on the plane of failure."

The statement that failure of a ductile material is by shear agrees with the later data; however, examination of data summarized in figure 9 shows that the normal component of the static stress did influence the permissible amplitude of alternating shear stress.

Bailey's method of analysis might be judged invalid because one of the basic assumptions, that is, that static normal stresses are of no influence, has been refuted; however, it deserves close inspection because, with his analysis, he made the prediction that static torsion

below a certain limit would have no effect on alternating bending, which was substantiated by Ono's test results (ref. 20). However, the analysis when applied to the effect of static torsion on alternating torsion (ref. 29) did not predict the known results presented in figure 6.

Other criteria for failure under combined alternating and static stresses are summarized in reference 30. They are all based upon the "Soderberg straight line law," which relates the permissible maximum stress S_{\max} to the absolute value of the mean stress $|S_m|$:

$$S_{\max} \leq (1 - \rho) |S_m| + S_e$$

$$\rho \equiv \frac{S_e}{S_{yp}}$$

where ρ is defined as the ratio of the reversed fatigue strength S_e to the yield strength S_{yp} .

The maximum-normal-stress criterion as presented in the present report consists of inserting each of the three principal stresses into the Soderberg law to see if the greatest principal stress is less than the expression on the right.

For the maximum-shear criteria, the Soderberg law is rewritten in terms of the shear stresses, and the maximum shear stress is limited:

$$\tau_{\max} \leq (1 - \rho) \tau_m \pm \frac{S_e}{2}$$

In the third criterion, the value of the distortion energies corresponding to the maximum stress, mean stress, and the reversed fatigue strength are inserted into the Soderberg law in place of the respective stresses.

The Soderberg law expresses the maximum of the stress cycle as a function of the absolute value of the mean stress; thus, it indicates that a static compressive stress reduces the permissible range of alternating stress as much as a static tensile stress does. The data presented in figure 5 show that a static compressive stress improves the permissible range of alternating stress instead of reducing it. Since all three of the above criteria, for the case of simple alternating axial stress superimposed upon a static stress, reduce to the statement of the Soderberg law, which has been shown not to agree with the

experimental data, their validity is questioned. The criteria do have utility in very conservative machine-design practice, but they mask the behavior present in the fatigue phenomenon.

EXPERIMENTAL CHECK ON PROPOSED CRITERION

Choice of Experimental Test

In the process of formulating the general stress criterion for fatigue, test results for various combinations of alternating stresses were examined and also those for combinations of simple static stresses with simple alternating stresses. Examination of the test results summarized in figure 9 reveals one notable absence, the effect of static compressive stress on alternating torsion. Test results were presented for the effect of static tensile stress on the permissible range of alternating torsion in figure 8 and were extrapolated into the compressive region; the dotted lines show the anticipated behavior.

It was decided to augment the existing data and to test the criterion by an experimental program. Specimens and a stressing system were designed and manufactured for the testing of two series of specimens, one with alternating torsion only and the other with static compressive stress superimposed on the alternating torsion.

Material

The material used for the test was 6061-T6 (61S-T6) aluminum alloy. This material was chosen for the test because its ratio of yield strength to fatigue strength is high; the occurrence of yielding from the combination of the applied torsion and compressive stresses would complicate the analysis of the results. The nominal properties (ref. 31) of the material are:

Ultimate tensile strength, psi	45,000
Yield strength, 0.2-percent offset, psi	40,000
Elongation in 2 in., percent	17
Brinell hardness, 500-kg load, 10-mm ball	95
Shear strength, psi	30,000
Reversed bending fatigue strength	17,000 psi at 10^7 cycles

The measured hardness was 89, which, when compared with the nominal value of 95, indicates that the yield strength might also be slightly less than the nominal.

Four specimens, approximately $3/4$ inch square, were machined from the width of 1- by 4-inch rolled plate.

Specimen

The specimen used to determine the effect of static compressive stress on alternating torsion is shown in a drawing (fig. 13) and in a photograph (fig. 14). The test sections are the two cylindrical surfaces that are separated by the short square length in the center. The alternating twisting moment is applied by the torque lever that clamps on this center section. The surfaces have a square cross section so that they can be clamped to resist the torsional moment. The cross-sectional area of the test section is less than that of the clamped surfaces so that failure occurs in the test section and not at a region under the influence of the unknown clamping stresses. The device used to apply the static compressive stress requires that a longitudinal hole be bored through the specimen.

For the convenience of holding the specimen in a collet chuck during machining, both ends of the specimen are turned to a diameter of $3/4$ inch for a $1/2$ -inch length.

The square clamped surfaces were trued by scraping and draw filing; their accuracy was checked by the transfer of bluing from a surface plate.

The final lathe cut was less than 0.005 inch and made with a sharp tool. Minnesota Mining and Manufacturing Co. Wetordry No. 240-, 320-, 400-, and 600-grit polishing paper was used with water to polish the test surface. Every specimen was polished circumferentially in a lathe and then longitudinally by hand with each grit. The longitudinal scratches were removed each time by the next finer paper, so that no scratches existed on the polished surface coarser than were left by the final paper, which had No. 600 grit.

Apparatus

Static compressing device.— The assembled device for applying the static compressive stress is presented in cross section in figure 15 and the disassembled components are shown in a photograph (fig. 14). The stress rod passes through the Belleville spring assembly and the hollow specimen. The spring and the specimen are compressed by tightening the hexagonal nut on the drawscrew. The outer disk is prevented from rotating during the tightening of the nut by a key that fits into a keyway on the drawscrew. All the parts are highly stressed, necessitating the use of hardened tool steels. The Belleville springs were machined into conical shape and then hardened before the final grinding to dimension. The

dimensions of the springs that are shown in figure 15 were calculated to give the desired range of compressive forces (ref. 32).

A number of advantages are derived from this application of Belleville springs because of their nonlinear force-deflection characteristics. The calibration curve for the spring assembly is given in figure 16. The calibration was performed by putting the assembled disks and springs between the compression heads of a Baldwin universal testing machine and measuring the deflection. The slope of the curve at the point of operation is very small; a 0.01-inch deflection corresponds to a change of only 50 pounds at the operating force of 2,720 pounds. This low slope permits a sufficiently accurate setting of the load without resorting to precise measurements in setting the deflection. If there should be any yielding of the projecting irregularities on the contacting surfaces of the end of the specimen or at the threads or any changes in relative length of the specimen and rod assembly from thermal or other causes, the low slope insures that only a negligible change in the load will result. Its nonlinearity and the mechanical simplicity permits the load to be set by using only a wrench, a scale divided in sixty-fourths of an inch, and outside calipers.

A danger inherent in applying an axial compressive load to a specimen is that an accidental eccentricity of the load will cause large undesired bending stresses. Stressing by means of a stress rod passing through the center hole of the specimen is used to avoid eccentric loading; the clearance between the rod and the hole bored through the specimen at the ends is less than 0.003 inch. The ends of the specimen onto which the load is applied were also machined within close tolerance to be square to the axis.

To insure against introducing bending by the clamping of the specimen in the fatigue machine and to cancel any bending stresses that might have been caused by eccentric loading, the clamped and clamping surfaces were finished straight and in line to within 0.0005 inch.

Fatigue testing machine.— The alternating torsional stress was applied to the specimen by a Krouse plate-bending fatigue machine modified to perform this particular test. A photograph of the modified machine is shown in figure 17 and the parts are identified in a sketch of the loading linkage (fig. 18). The adjustable crank is fastened to the shaft of a 1,750-rpm induction motor. A connecting rod applies the crank eccentricity to a horizontal torque arm, the other end of which clamps to the center of the torsion specimen. The vise that grips the ends of the torsion specimen is seen at the left in the photograph, behind which can be seen the disk-shaped Belleville springs used to apply the compressive prestress.

At the top of the specimen vise is a screw used to adjust the vertical distance between the specimen and the motor. This distance determines the static torque that is applied to the specimen.

An arrangement had to be designed to shut off the machine when a fatigue failure occurred. It was not expected that the specimens would break in half, so the switch had to be sensitive enough to be actuated by the formation of a fatigue crack. The torque lever as shown in figure 18 has considerable elastic deflection in the extreme stress position shown. When a crack of sufficient length appears, the torsional rigidity of the specimen is reduced and the elastic deflection of the torque arm is less for the same eccentric throw. The arm straightens as illustrated by the dotted line and its lower surface touches a mechanical contact and trips a microswitch to shut off the motor. A counter attached to the rear of the motor records the number of cycles to failure.

Method of Setting Stresses

Static compressive stress.- The static compressing device is attached to the specimen by sliding the rod of the Belleville spring assembly through the hole of the specimen and then screwing the end nut onto the rod as shown assembled in figure 15. The assembly is then placed in a machinist's vise and gripped on the flats provided for this purpose on the end of the drawscrew; thus held, the hexagonal nut on the drawscrew is tightened by a wrench. The setting was closer than ± 0.01 inch, which gives an accuracy in load of ± 50 pounds in 2,720 pounds or 1.8 percent.

Torsional stresses.- The fatigue specimen, subjected to static compressive stress by the attached prestressing device, is inserted between the two halves of the specimen clamp and the eight clamping bolts are uniformly tightened. The torque arm is then clamped onto the square center section of the specimen.

The stresses are set by reproducing deflections determined from dead-weight loadings. A device is attached to the machine during the setting of the stress to indicate the deflections. The long arm of this device is attached to the bottom of the specimen clamp by means of a C clamp as shown in figure 19. A contact screw at the end of the arm is electrically insulated from the testing machine. The screw can be turned so that its conical point contacts the torque arm. An electronic indicator shows when electrical contact is made.

Two adjustments must be made to set the torsional stress: (1) The vertical position of the vise to fix the static torsional stress, and (2) the throw of the adjustable crank to fix the alternating stress:

(1) The static torsional stress, which in all these tests was zero, is set first. With the connecting-rod pin removed and the connecting rod swung free from the torque arm, the contact screw is set to touch

the torque arm. This deflection corresponds to a zero static stress; if the static torsional stress desired is other than zero, a weight to give that stress is hung from the torque arm at the connecting-rod pin. With the crank set for zero throw, the connecting rod is attached to the torque arm by inserting the connecting-rod pin. The height of the vise is then adjusted so that contact is just made with the screw. The vise locking screws are then tightened to hold the setting.

(2) The alternating stress is set next. The connecting-rod pin is disconnected and swung aside and the weight pan is attached to the torque arm at the connecting-rod pin. Using the weight corresponding to the maximum torsional stress of the fatigue cycle, the contact screw is set to make contact. The weight pan is removed and the connecting rod attached. The crank throw is adjusted to reproduce the deflection as determined from the application of dead weight. A locking screw on the crank is tightened to hold this adjustment.

The stresses having been set, the indicator arm and screw are removed. After the cycle counter is read, the machine is turned on and the shutoff switch set. The switch is set so that contact is not quite made between it and the torque arm but so that a few pounds of force (e.g., the weight of a hand placed on the center of the torque arm) will cause enough deflection to trip the switch.

Test Results

The results of the fatigue tests are presented in table 1, and in figure 20 the amplitude of the alternating torsional stress is plotted against the logarithm of the number of stress cycles that caused failure. Two parallel straight lines nicely fit the two series of fatigue data. The curves are separated sufficiently so that the scatter for the two curves does not overlap. At 10^7 cycles, which is a lifetime commonly used for comparison, the amplitude of the torsional stress is 13,000 psi (probable error, ± 500 psi) and when the static compressive stress of 21,700 psi was superimposed on the torsional stress, its amplitude was increased to 15,000 psi (probable error, ± 500 psi).

The specimens did not fail by complete rupture but by the formation of very narrow longitudinal cracks in the test section. A crack of about $1/4$ inch in length was sufficient to shut off the machine. The cracks were so fine that they could scarcely be seen with the naked eye. Some of the specimens cracked in both test sections. The test on specimen 2 was continued until the crack extended into the fillet at the end of the test section. In the fillet, the crack branched into a circumferential crack and also continued longitudinally. Black powder formed by attrition of the surface of the crack marked the intersection of the crack with the bore, thus revealing that the cracks extended through the test section.

Discussion of Test Results

It is interesting that the fatigue cracks formed along planes of maximum alternation of shear stress because the combined-alternating-stress data cited earlier in the report indicate that it is the alternation of shear stress that causes the failure. However, this observation of the direction of propagation of the fatigue crack can hardly be taken as an indication of the fracture mechanism, for other investigators (refs. 33 and 34) have observed that cracks caused by torsional stresses often propagate normal to the maximum normal stress. Perhaps it is the orientation of the flaw from which the crack initiates that determines the direction of the propagation and the flaws might have acquired a preferred orientation during the rolling process.

The formation of a longitudinal crack was delayed by a longitudinal compressive stress, although it has no component on the plane of the crack. This lends support to the criterion which states that it is the sum of the orthogonal components of the normal static stress that is effective, because no direction can be attributed to the arithmetic sum.

The presence of microscopic residual stresses in the specimen is unlikely because the test section of 0.50-inch outside diameter and 0.30-inch inside diameter was machined from the 1- by 4-inch stock. It is difficult to imagine residual-stress gradients at the center of the 1-inch thickness so steep that they would not be relieved by the machining.

The experimental results for the effect of static compressive stress are compared in figure 21 with the curves for the effect of static stress that have been extrapolated in the way predicted by the general stress criterion. It is seen that the data agree closely with the predicted behavior, although the tests under compression were performed on a metal different from that tested under tension.

Most of the test data examined have been limited to cases in which the yield strength was not exceeded. The behavior revealed by the test data may be very different from that predicted by the general criterion if yielding occurs, as can be seen by the sudden drop of permissible alternation of stress shown in figures 6 and 7(b), where the yield strength was exceeded under other combinations of stresses.

MODIFICATION OF OROWAN THEORY OF FATIGUE

TO INCLUDE EFFECT OF STATIC STRESS

The experimental information on the effect of static stresses on the permissible range of alternating stress is generalized by the mathematical

statement of the criterion. A valid theory of fatigue should agree with this generalization of the known behavior. Orowan proposed a semiquantitative theory of fatigue in 1939, which will be examined to see whether the mechanism of failure advanced in it is compatible with the criterion (ref. 35).⁴

Orowan's analysis predicts many aspects of the behavior of metals under repeated stress; he outlines them as follows:

"(1) The quasi-brittle nature of fatigue fracture. A metal, however ductile, can break in a fatigue test without any appreciable external deformation, like a brittle material. A further similarity to brittle fracture is that fine cracks and other faults, which would not influence noticeably the static strength of a ductile material, substantially impair its fatigue endurance.

"(2) Internal distortions. In spite of the possible absence of any external deformation, heavy local distortions can be observed microscopically on a material subjected to a fatigue test. The evidence for internal distortions has been extended by the X-ray work of Gough and his collaborators, who found that X-ray photographs of fatigue-fractured metals show, in the immediate neighbourhood of the fatigue crack, qualitatively and quantitatively the same alterations as those of metals fractured in static tests.

"(3) Existence of safe ranges. The algebraic difference between the maximum and the minimum stress of the cycle is called the range of stress. For a fixed mean stress of the cycle, the number of cycles that the material can withstand increases rapidly with decreasing range of stress. For applications in engineering it is of the highest importance that, in most cases, a limiting range of stress exists below which the material will withstand any number of cycles. By plotting the results of fatigue tests as log S-log N curves a characteristic fact is revealed: In general, this curve consists of two straight parts, one inclined (representing the unsafe ranges) and one practically horizontal (representing the behavior of the material at the limiting safe range). The transition between the two straight parts is more or less rounded off."

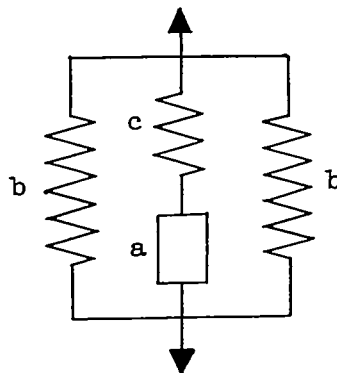
However, the theory predicts that static stress should have no effect on the permissible range of alternating stress. Although some experimental evidence, which indicates that the effect of the static stress is very small or even negligible, is cited in the paper, the large collection of experimental evidence presented in earlier sections of the present paper reveals an appreciable effect of the static stress. Orowan's analysis

⁴The effect of mean stress has already been considered in another theory of fatigue presented by Shanley in reference 36. Experimental evidence to distinguish which of these two theories more closely describes the phenomenon is not existent.

will be discussed briefly to see whether it is amenable to a modification that will introduce the effect of the static stress.

Orowan's theory is based upon the relation between the stress and the plastic strain existing at microscopic inhomogeneities within the material. He cites several experiments that show that localized plastic strain does occur under repeated stresses that are beneath the yield strength of the material. A stress that would not cause yielding of the bulk of the material may cause the stress produced by a microscopic inhomogeneity to reach the yield strength and cause plastic flow, because of the stress concentration of the homogeneity. The plastic flow limits the stress to that stress at which the flow occurs for the material in that region. As the stress is repeated, the plastic region work-hardens and the stress to cause the yielding must increase. If the ability to flow is exhausted and if the applied stress and the stress concentration of the inhomogeneity are great enough, the stress on the microscopic region will exceed its rupture strength and a crack will form. After the plastic deformation stops, the localized stress may not have exceeded the rupture strength and then the stress can be applied repeatedly without leading to failure.

Orowan idealizes the action of the microscopic plastic region embedded in its elastic surroundings by the following model:



Sketch 2

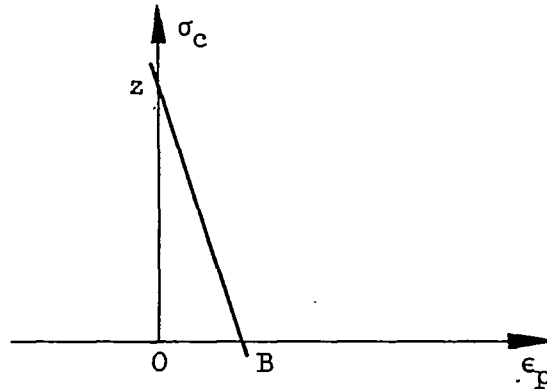
The model consists of a plastic element a in series with a spring c , the assembly being in parallel with the springs b , which represent the elastic surroundings.

From the two considerations (1) that the total unit stress is the sum of the forces on the plastic element and the parallel elastic element and (2) that the elongation of the series element a together with c must equal that of b , a linear equation between the plastic strain of the element ϵ_p and the stress σ_c acting upon it can be derived.

This relation is

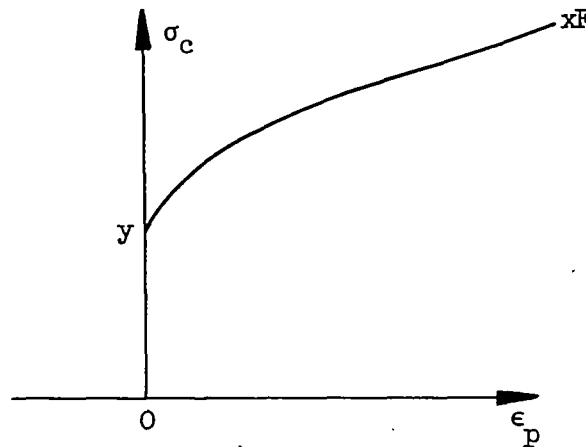
$$\sigma k_1 = \sigma_c + k_2 \epsilon_p \quad (1)$$

In which k_1 and k_2 are constants and σ is the applied stress. This functional relation can be plotted in the following manner:



Sketch 3

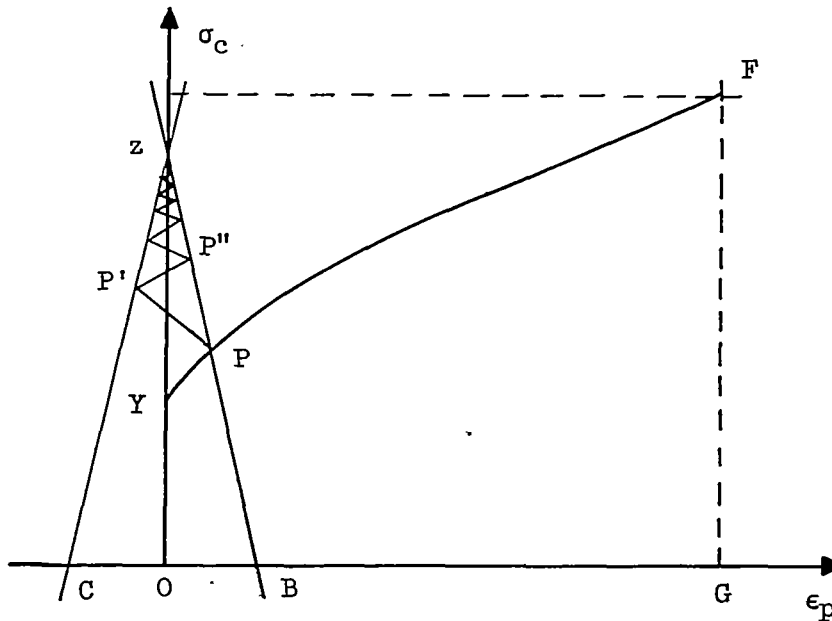
The work-hardening curve for the hypothetical plastic element gives another relation between the stress σ_c and the plastic strain ϵ_p :



Sketch 4

These two relations between the strain and stress for the plastic element must be satisfied when alternating stresses are applied to the material. When a periodically reversed, uniaxial stress σ is applied to a specimen, the stress and strain for the plastic element follow the work-hardening curve OYF of sketch 5, until halted at point p, the intersection with line BZ which represents the other relation between the stress and strain. Assuming that stressing in compression causes the same work-hardening as stressing in tension, the application of the

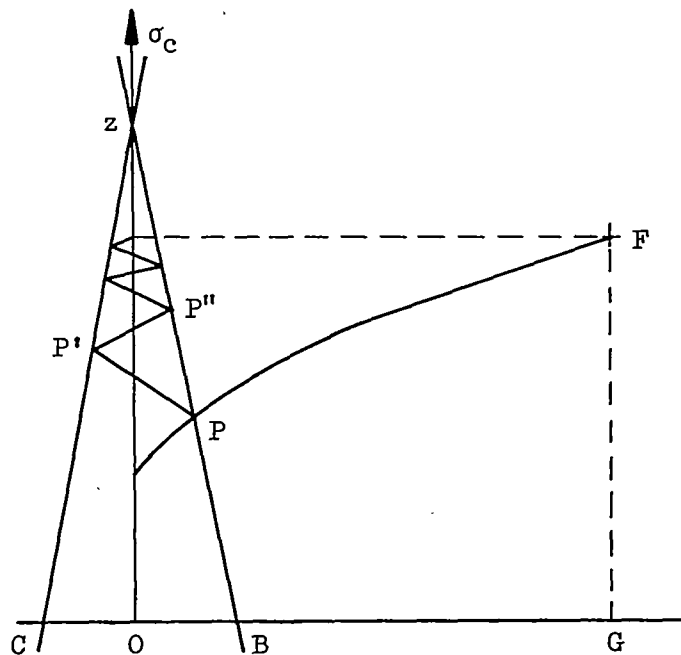
reversed stress causes the stress to rise, and the strain to reverse, over path PP' . (The ordinate represents the absolute value of the stress



Sketch 5

on the plastic element.) Path PP' is the strain-hardening curve reflected about a vertical line passing through P . On the next cycle, the tensile stress increases and the strain increases until P'' is reached; $P'P''$ is the segment of the strain-hardening curve that had been reflected about the vertical through P and is now again reflected about the vertical through P' . During subsequent cycles, the stress rises along a zigzag curve enclosed between the lines of the triangle ZB and ZC , which express the stress-strain relation, equation (1). Whatever the shape of the strain-hardening curve may be, the zigzag curve cannot rise above the apex of the triangle, point Z . If the fracture strength of the element is greater than OZ , then no failure can occur no matter how many cycles of stress are applied. However, if the amplitude of the applied alternating stress σ is great enough so that OZ exceeds the fracture strength FG , then, after

a certain number of repetitions, the stress will exceed the fracture strength and a fatigue crack will start (sketch 6).



Sketch 6

Without the insertion of any additional information on the variation of any of the parameters with static stress, the theory is shown by Orowan to predict that static stresses should have no effect on the permissible range of stress below the elastic limit. The tests quoted in an earlier section of the paper, and particularly those of Roš and Eichinger (ref. 5) and Smith (ref. 14), show that this is the case when the static stress is shear but that static normal stresses have no appreciable effect.

Orowan's statement that the limiting safe range depends only on the strength of the plastic region and on the "stress concentration" factor should be emphasized. More specifically, the mechanism of fatigue outlined by Orowan states that the safe range is determined by the strength attained by the plastic region in the most severely work hardened condition that can be obtained by the action of alternating strains to a region confined by the elastic surroundings and the nature of the inhomogeneity. The question now arises as to what gross static measurement is most closely associated with this strength property of the plastic element of the model.

The ultimate strength, which is the maximum static load divided by the original undeformed cross-sectional area, seems to have little connection with the mechanism because there may be considerable reduction in cross-sectional area before fracture occurs. The "true strength," which is defined as load at fracture divided by the actual fractured

area, has more significance; however, the situation is complicated by the complex stress condition present across the necked section. Bridgman (ref. 37) removes the complication by introducing the concept of "final flow stress," which he defines as the longitudinal normal stress on the outer surface of the neck at the time of rupture. From experimental and mathematical considerations, he obtains the stress-strain conditions present in the neck that are needed to calculate the flow stress.

The final-flow-stress description of the strength property of a material has more significance than the others because, in it, consideration has been taken of the actual stresses present at the failure region in the static test. However, it still is not exactly the "strength of the plastic region" mentioned in Orowan's analysis because its work-hardened state was obtained by a single application of a unidirectional load and it underwent necking, while the plastic region was subjected to alternating strains and was confined. A correlation between the two properties seems likely.

Even if the final flow stress was the rupture strength of the plastic region, computation of the fatigue strength from the final flow stress for various materials would not be possible because the nature of the inhomogeneity effective in the fatigue failure is not known. However, factors that cause a variation in the flow stress without affecting the structure of the material should also cause a comparable change in the limiting safe fatigue strength.

The ultimate strength, true rupture strength, and the final flow stress are all influenced by hydrostatic pressure in a manner similar to that in which static normal stresses affect fatigue failure. In table 2 some typical test results for the effect of hydrostatic pressure on the true strength and the final flow stress are presented. The values called the "pressure coefficients"⁵ given in the table are the ratios of the change in true stress corresponding to a change in hydrostatic pressure and of the change in final flow stress corresponding to the change in hydrostatic pressure. These were obtained by plotting the data, fitting a straight line to the points, and measuring the slope. The data have considerable scatter, but a definite functional relation with the hydrostatic pressure is evident.

The changes in final flow stress corresponding to the changes in hydrostatic pressure for the steels presented in table 2 are 0.90, 0.90, 0.60, and 0.80, which average 0.80 ± 0.08 . The changes in permissible stress amplitude corresponding to the applied uniaxial mean stress are 0.22, 0.24, and 0.25 for Nishihara's steels (see fig. 5), averaging 0.237 ± 0.009 ; 0.23 for Roß's low-carbon steels; and 0.20 for Newmark's tests on 2024-T (24S-T) aluminum. These numbers are values for α , the

⁵Note that this "pressure coefficient" is different from that commonly used in the field of high-pressure physics.

coefficient of the sum of the orthogonal static stress components, which appears in the proposed stress criterion for fatigue. If the static stress is expressed in terms of the hydrostatic pressure, the new coefficient is $3 \times \alpha$, thus making the average value for the hydrostatic pressure coefficient $3 \times 0.237 = 0.71 \pm 0.03$. The value of 0.71 for the pressure coefficient for fatigue is close to the value of 0.80 for the pressure coefficient for the final flow stress for a similar material. This may indicate that the final flow stress (the refined rupture strength defined by Bridgman) has a close relation to the "strength of the plastic region" appearing in Orowan's analysis.

Although the comparison was made using hydrostatic stress, it is not intended to limit the effect to the action of the hydrostatic (equi-triaxial) stress state. The flow on the plane on which slip occurs is affected by the normal stress on that plane and the normal stress can result from the application of either uniaxial, biaxial, or triaxial static stresses. Bridgman suggested (private correspondence) that this can be shown by the data in chapter 15 of his book (ref. 37). Here the effect of a uniaxial compressive stress on maximum torsional strength is presented. The uniaxial pressure coefficient, the change in maximum shear strength corresponding to the change in compressive stress, is 0.21. (The final flow stress in the torsional test is equal to the maximum shear stress.) This coefficient 0.21 can be compared directly with the uniaxial pressure coefficients for fatigue of 0.22, 0.24, 0.25, and 0.20 mentioned above. Pressure coefficients cannot be obtained from the other tests on the effect of a uniaxial compressive stress on torsion presented in Bridgman's book because of the uncertainty in the diameter of the test section caused by the yielding.

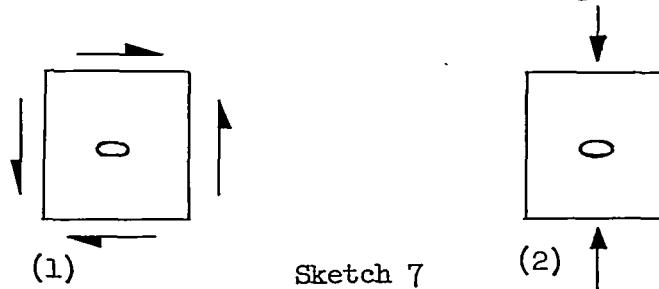
The above considerations make it reasonable to insert the dependence of the strength of the plastic region upon the static normal stress into the Orowan theory. When static compressive stresses are applied during plastic deformation, the fracture strength of the plastic element represented by GF in sketch 6 is increased, thereby raising the fatigue strength. It is inferred that deformation under tensile stress reduces GF and thereby the fatigue strength. With this modification, the theory predicts the experimentally revealed effect that static stress has upon the permissible amplitude of alternating stress.

University of California,
Los Angeles, Calif., March 24, 1954.

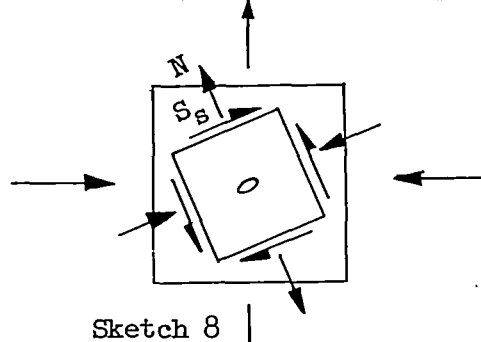
APPENDIX A

ANALYSIS OF STRESSES AT CRACKS OF VARIOUS ORIENTATIONS

An examination will be made of cracks oriented at different angles under several combinations of stress to find the maximum localized stresses that occur in each case. The shape of the crack is assumed to be a much elongated elliptical hole, because the stresses about this shape have been solved by Neuber and are presented in a graphical form in his book (ref. 38) and because this shape is a reasonable idealization of a flakelike hole. He has solved the case in which the volume containing the hole is subjected to pure shear (1) and also the case for tension (2). (The dimensions of the volume are large compared with those of the hole.)



The general stress state applied to the body containing the hole can be expressed by shear and normal stresses, which act on planes enclosing the hole and are oriented parallel and perpendicular to its axes:



At the hole, the localized stresses caused by the shear component can be superimposed on those arising from the normal component; this superposition is permissible by the theory of elasticity because the deformations are small.

The shear and normal components S_s and N which act on the enclosing planes in the above sketch were found graphically by use of the Mohr circle (ref. 23) for several different orientations and stress states. The normal stress parallel to the major axis of the hole was not found

because it makes no appreciable contribution to the stress at the end of the hole.

Figure 22(a) shows the value of the normal stress at the surface of the hole, parallel to its surface, which results from a tensile stress applied to the element. Note that the surface stress reaches a maximum at the end of the hole on the x-axis. The normal stress on the x-axis is shown on the right as a function of the distance away from the edge of the hole.

The stresses caused by pure shear applied to the element are shown in figure 22(b). The normal stress parallel to the surface reaches a maximum at a point on it that is 45° to the axes. On the right is shown the maximum shear that acts on the x-axis. However, this is not the greatest shear stress; it occurs at the same point on the surface where the normal stress is greatest.

The local stress, which results from the superposition of the local stresses caused by the applied shear and normal stress components, is great at two points. One point is on the x-axis, a short distance beneath the surface, where the maximum shear stress caused by the applied shear stress component adds to the localized normal stress caused by the applied normal stress component. The other highly stressed point is at the surface of the hole, near the end of the hole, where the sum of the localized normal stresses caused by the applied shear and applied normal stress components reaches a maximum. The local combined shear and normal stresses for the first point were calculated by means of the Mohr circle and the combination was found to be less than that for the other point, which is on the surface.

The maximum stresses were found by the following method and are presented in table 3. The effect of stress state A, identified in the table, on the crack oriented in position 2 will be determined as an example.

The stresses caused by σ_1 on planes enclosing the hole, parallel and normal to its axes, were found by means of the Mohr circle. The normal stress N , which is given in the second column, is equal to $0.85\sigma_1$, and the shear stress S_s , which is in the third column, is equal to $0.35\sigma_1$. The local stresses caused by the shear components given in figure 22(a) and those caused by the normal component given in figure 22(b) were multiplied by these fractions, 0.85 and 0.35, respectively, and then added graphically to find the maximum local stress at the notch. The maximum stress for this case was found to be on a plane whose normal makes about a 20° angle with the x-axis, and this maximum sum was $11\sigma_1$. The shear stress at the surface is equal to one-half the normal stress, that is, $5.5\sigma_1$.

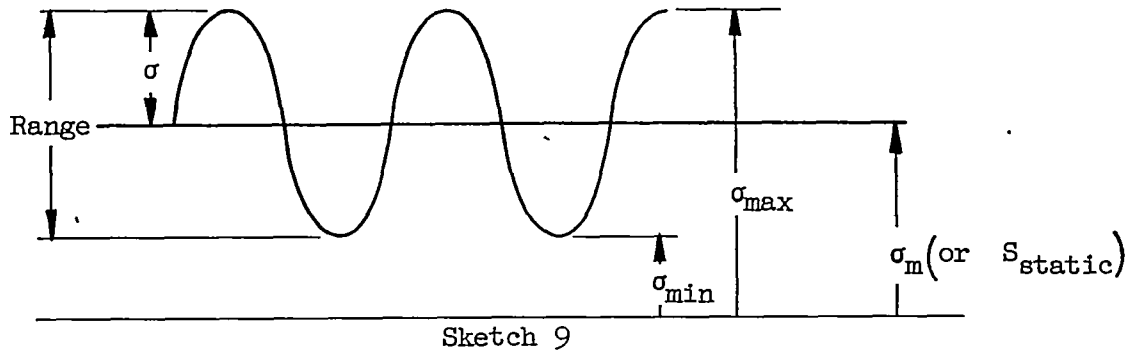
This process was repeated for the five crack orientations and the three stress states. In all cases, except for orientations 2 and 4 with stress state C, the greatest value of stress was the same ($11\sigma_1$ for the normal and $5.5\sigma_1$ for the shear). For the one exception, in which the transverse and longitudinal stress were equal in magnitude, the maximum stresses were slightly higher (normal stress equal to $13\sigma_1$ and the shear stress equal to $6.5\sigma_1$).

Thus, it is seen that the maximum of the localized stresses at the elongated holes is determined by the greater in magnitude of the applied principal stresses and is but slightly influenced by the secondary stress.

APPENDIX B

TRANSFORMATION OF GENERAL CRITERION INTO TERMS OF
MAXIMUM AND MINIMUM STRESS RATIO

The transformation of the general criterion into terms of maximum and minimum stress ratio is as follows:



Commonly, the stress cycle is described by R :

$$R \equiv \frac{\sigma_{\min}}{\sigma_{\max}}$$

The half range σ is given by

$$\begin{aligned}\sigma &= \frac{\sigma_{\max} - \sigma_{\min}}{2} \\ &= \frac{\sigma_{\max}(1 - R)}{2}\end{aligned}$$

and the mean stress S is

$$\begin{aligned}S &= \frac{\sigma_{\max} + \sigma_{\min}}{2} \\ &= \frac{\sigma_{\max}(1 + R)}{2} \\ &= \frac{2}{1 - R} \sigma \frac{1 + R}{2} \\ &= \frac{1 + R}{1 - R} \sigma\end{aligned}$$

Define

$$m \equiv \frac{1 + R}{1 - R}$$

The normal form of the general criterion is as follows, where σ 's are the amplitudes of the alternating principal normal stresses:

$$\frac{1}{3} \sqrt{(\sigma_1 - \sigma_2)^2 + (\sigma_2 - \sigma_3)^2 + (\sigma_1 - \sigma_3)^2} = A - \alpha (S_x + S_y + S_z)$$

At the surface $\sigma_3 = 0$ so that

$$\frac{1}{3} \sqrt{2\sigma_1^2 - 2\sigma_1\sigma_2 + 2\sigma_2^2} = A - \alpha (S_x + S_y + S_z)$$

Now

$$S = m\sigma$$

where

$$m \equiv \frac{1 + R}{1 - R}$$

and

$$\frac{1}{3} \sqrt{2\sigma_1^2 - 2\sigma_1\sigma_2 + 2\sigma_2^2} = A - \alpha m (\sigma_1 + \sigma_2)$$

$$\begin{aligned} \sigma_1^2 - \sigma_1\sigma_2 + \sigma_2^2 &= \frac{9}{2} \left[A - \alpha m (\sigma_1 + \sigma_2) \right]^2 \\ &= \left[a - b m (\sigma_1 + \sigma_2) \right]^2 \end{aligned}$$

where

$$a = \frac{3}{\sqrt{2}} A$$

$$b = \frac{3}{\sqrt{2}} \alpha$$

Reduced to standard form for conic sections,

$$A\sigma_1^2 + B\sigma_1\sigma_2 + C\sigma_2^2 + D\sigma_1 + E\sigma_2 + F = 0$$

where

$$A = C = 1$$

$$B = -\frac{1 + b^2 m^2}{\left(1 - \frac{b^2 m^2}{2}\right)}$$

$$D = E = \frac{abm}{\left(1 - \frac{b^2 m^2}{2}\right)}$$

$$F = \frac{a^2}{2\left(1 - \frac{b^2 m^2}{2}\right)}$$

For the stress cycle where $\sigma_1 = S_x$, $\sigma_2 = S_y$, and $\sigma_3 = S_z$, m is unity.

REFERENCES

1. Gough, H. J.: Some Experiments on the Resistance of Metals to Fatigue Under Combined Stresses. R. & M. No. 2522, British A.R.C., 1951.
2. Findley, W. N.: Fatigue of 76S-T61 Aluminum Alloy Under Combined Bending and Torsion. Proc. A.S.T.M., vol. 52, 1952, pp. 818-833.
3. Puchner, O.: Zur Dauerhaltbarkeit von Formelementen der Welle bei ueberlagerter wechselnder Beige- und Verdrehbeanspruchung. Schweizer Archiv angewandte Wiss. und Technik, Bd. 14, Nr. 8, Aug. 1948, pp. 217-229.
4. Sawert, Walter: Verhalten der Baustähle bei wechselnder mehrachsiger Beanspruchung. Z.V.D.I., Bd. 87, Nr. 39/40, Oct. 2, 1943, pp. 609-615.
5. Roš, M., and Eichinger, A.: Die Bruchgefahr fester Körper bei wiederhalten Beanspruchung-Ermüdung. Metalle. Bericht 173, Eidgenossische Materialprüfungs- und Versuchsanstalt für Industrie, Bauwesen und Gewerbe (Zurich), Sept. 1950.
6. Maier, A. F.: Wechselbeanspruchung von Rohren unter Innendruck. Stahl und Eisen, Bd. 54, Heft 50, Dec. 13, 1934, pp. 1289-1291.
7. Sachs, G.: Zur Ableitung einer Fließbedingung. Z.V.D.I., Bd. 72, Nr. 22, June 2, 1928, pp. 734-736.
8. Hencky, Heinrich: Zur Theorie plastischer Deformationen und der hierdurch im Material hervorgerufenen Nachspannungen. Z.a.M.M., Bd. 4, Heft 4, Aug. 1924, pp. 323-334.
9. Battelle Memorial Institute: Prevention of the Failure of Metals Under Repeated Stress. John Wiley & Sons, Inc., 1941, pp. 115-117.
10. Turner, L. B.: The Strength of Steels in Compound Stress and Endurance Under Repetition of Stress. Engineering, vol. XCII, Aug. 25, 1911, pp. 247-250.
11. Sisco, Frank T.: Modern Metallurgy for Engineers. Second ed., Pitman Pub. Corp. (New York), 1948.
12. Thum, A., and Petersen, C.: The Fatigue Strength of Cast Iron. Archiv Eisenhüttenwesen, Bd. 16, Heft 8, Feb. 1943, pp. 309-312.
13. Nishihara, Toshio, and Sakurai, Tadakazu: Fatigue Strength of Steel for Repeated Tension and Compression. Trans. Soc. Mech. Eng. (Japan), vol. 5, no. 18, Feb. 1939, pp. I-25 - I-29. (Text in Japanese. English summary, pp. S-8 - S-9.)

14. Smith, James O.: The Effect of Range of Stress on the Fatigue Strength of Metals. Bull. No. 334, Eng. Exp. Station, Univ. of Ill., vol. 39, no. 26, Feb. 17, 1942.
15. Newmark, N. M., Mosberg, R. J., Munse, W. H., and Elling, R. E.: Fatigue Tests in Axial Compression. Proc. A.S.T.M., vol. 51, 1951, pp. 792-803; discussion, pp. 803-810.
16. Ludwik, P., and Krystof, J.: Einfluss der Vorspannung auf die Dauerfestigkeit. Z.V.D.I., Bd. 77, Nr. 24, June 17, 1933, pp. 629-635.
17. Moore, H. F., and Lewis, R. E.: Fatigue Tests in Shear of Three Non-Ferrous Metals. Proc. A.S.T.M., vol. 31, pt. 2, 1931, pp. 236-242.
18. Gough, H. J., and Pollard, H. V.: The Strength of Metals Under Combined Alternating Stresses. Proc. Institution Mech. Eng. (London), vol. 131, Nov. 1935, pp. 1-103.
19. Lea, F. C., and Budgen, H. P.: Combined Torsional and Repeated Bending Stresses. Engineering, vol. CXXII, Aug. 20, 1926, pp. 242-245.
20. Ono, Akimasu: Fatigue of Steels Under Combined Bending and Torsion. Memoirs, College of Eng., Kyushu Imperial Univ., vol. II, no. 2, 1921, pp. 117-142.
21. Nimhanminne, S. K.: The Failure of Material Under Constant Torsion and Alternating Bending. Master's Thesis, Battersea Polytechnic Inst., 1931.
22. Huitt, W. J.: The Failure of Nickel Alloy Steel Under Torsion by the Addition of Alternating Bending. Master's Thesis, Battersea Polytechnic Inst., May 1935.
23. Timoshenko, S.: Theory of Elasticity. McGraw-Hill Book Co., Inc., 1934, p. 187.
24. Hill, R.: The Mathematical Theory of Plasticity. The Clarendon Press (Oxford), 1950, p. 17.
25. Marin, Joseph, and Shelson, William: Biaxial Fatigue Strength of 24S-T Aluminum Alloy. NACA TN 1889, 1949.
26. Morikawa, G. K., and Griffis, L.: The Biaxial Fatigue Strength of Low-Carbon Steels. The Welding Jour., vol. 24, Mar. 1945, pp. 167-s - 174-s.

27. Bailey, R. W.: Ductile Materials Under Variable Shear Stress. Engineering, vol. CIV, July 27, 1917, pp. 81-83.
28. Stanton, T. E., and Batson, R. G.: On the Fatigue Resistance of Mild Steel Under Various Conditions of Stress Distribution. Engineering, vol. CII, Sept. 15, 1916, pp. 269-270.
29. Sines, George: Failure of Materials Under Combined Repeated Stresses With Superimposed Static Stresses. Ph. D. Thesis, Univ. of Calif., Los Angeles, Aug. 1953.
30. Marin, J.: Engineering Materials. Prentice-Hall, Inc., 1952.
31. Anon.: Alcoa Aluminum and Its Alloys. Aluminum Co. of Am. (Pittsburgh), 1950.
32. Anon.: Handbook of Mechanical Spring Design. Associated Spring Corp. (Bristol Conn.), 1951.
33. Southwell, R. V., and Gough, H. J.: On the Concentration of Stress in the Neighbourhood of a Small Spherical Flaw; and on the Propagation of Fatigue Fractures in "Statistically Isotropic" Materials. London, Dublin, and Edinburgh Phil. Mag. and Jour. Sci., ser. 7, vol. 1, no. 1, Jan. 1926, pp. 71-97; also R. & M. No. 1003, British A.R.C., 1926.
34. Smith, James O.: The Effect of Range of Stress on the Torsional Fatigue Strength of Steel. Bull. No. 316, Eng. Exp. Station, Univ. of Ill., vol. 33, 1939.
35. Crowan, E.: Theory of the Fatigue of Metals. Proc. Roy. Soc. (London), ser. A, vol. 171, no. 944, May 1, 1939, pp. 79-106.
36. Shanley, F. R.: A Theory of Fatigue Based on Unbonding During Reversed Slip. P-350, The Rand Corp., Nov. 11, 1952; Supplement, May 1, 1953.
37. Bridgman, P. W.: Studies in Large Plastic Flow and Fracture With Special Emphasis on the Effects of Hydrostatic Pressure. First ed., McGraw-Hill Book Co., Inc., 1952, Ch. 1.
38. Neuber, H.: Theory of Notch Stresses: Principles for Exact Stress Calculation. J. W. Edwards (Ann Arbor, Mich.), 1946.
39. Nishihara, Toshio, and Kojima, Kohei: Diagram of Endurance Limit of Duralumin for Repeated Tension and Compression. Trans. Soc. Mech. Eng. (Japan), vol. 5, no. 20, Aug. 1939, pp. I-1 - I-2. (Text in Japanese. English summary, p. S-67.)

40. Hankins, G. A.: Torsional Fatigue Tests on Spring Steels. Special Rep. No. 9, Eng. Res., Dept. Sci. and Ind. Res. (Gr. Brit.), 1929.
41. Pomp, A., and Hempel, M.: Das Verhalten von Gusseisen unter Zug-Druck-Wechselbeanspruchung. Stahl und Eisen, Bd. 57, Heft 40, Oct. 1937, pp. 1125-1127.
42. Johnson, J. B.: Fatigue Characteristics of Helical Springs. The Iron Age, vol. 133, no. 11, Mar. 15, 1934; no. 12, Mar. 22, 1934, pp. 24-26.
43. Moore, H. F., and Jasper, T. M.: An Investigation of the Fatigue of Metals. Bull. No. 142, Eng. Exp. Station, Univ. of Ill., vol. 21, no. 37, May 26, 1924, p. 60.
44. McAdam, D. J., Jr.: The Endurance Range of Steel. Proc. A.S.T.M., vol. 24, pt. 2, 1924, pp. 574-600.
45. Hohenemser, K., and Prager, W.: The Problem of Fatigue Strength Under Complex Stresses. Metallwirtschaft, Bd. XII, Heft 24, June 24, 1933, pp. 342-343.

TABLE 1

TEST RESULTS

[Inside diam., 0.298 in.]

Specimen	Outside diam., in.	Weight at 20-in. lever arm, lb	Cycles to failure
1	0.4974	17	2,082,000
2	.4985	15	4,354,000
3	.4980	19	390,000
4	.4983	19 (compressed)	1,066,000
5	.4967	17 (compressed)	4,241,000
6	.4961	15 (compressed)	15,436,000
7	.4954	16 (compressed)	7,038,000
8	.4975	14	14,552,000
9	.4964	18 (compressed)	2,103,000
10	Destroyed	-----	-----
11	.4975	$16\frac{1}{2}$ (compressed)	8,756,000
12	.4966	16	2,190,000
13	.4965	$14\frac{1}{2}$	4,813,000

TABLE 2
EFFECT OF HYDROSTATIC PRESSURE ON TRUE RUPTURE STRENGTH

[Data from ref. 37]

	True strength	Final flow stress
1-0 steel, ^a as received		
Applied pressure, psi:		
Atmospheric	169	146
40×10^3	219	164
140	385	284
Pressure coefficient	1.60	0.90
2-0 steel, ^b as received		
Applied pressure, psi:		
Atmospheric	191	169
54×10^3	250	204
117	314	236
188	470	340
Pressure coefficient	1.50	0.90
2-1 steel, ^b normalized at 1,650° F for 1/2 hr		
Applied pressure, psi:		
Atmospheric	197	166
53×10^3	-- 256	204
87	320	247
168	296	221
Pressure coefficient	1.50	0.60
2-2 steel, ^b annealed, fine-grained, at 1,500° F for 1/2 hr		
Applied pressure, psi:		
Atmospheric	174	150
58×10^3	213	170
201	422	314
Pressure coefficient	1.30	0.80

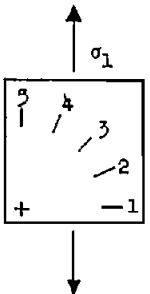
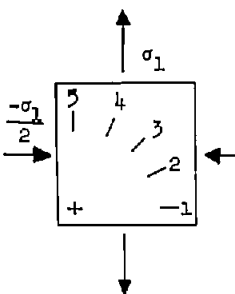
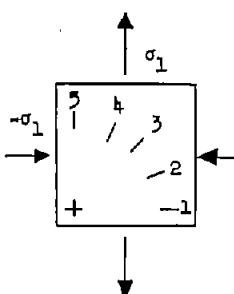
^aComposition: 0.34 carbon, 0.75 molybdenum, 0.017 phosphorus, 0.033 sulfur, and 0.18 silicon.

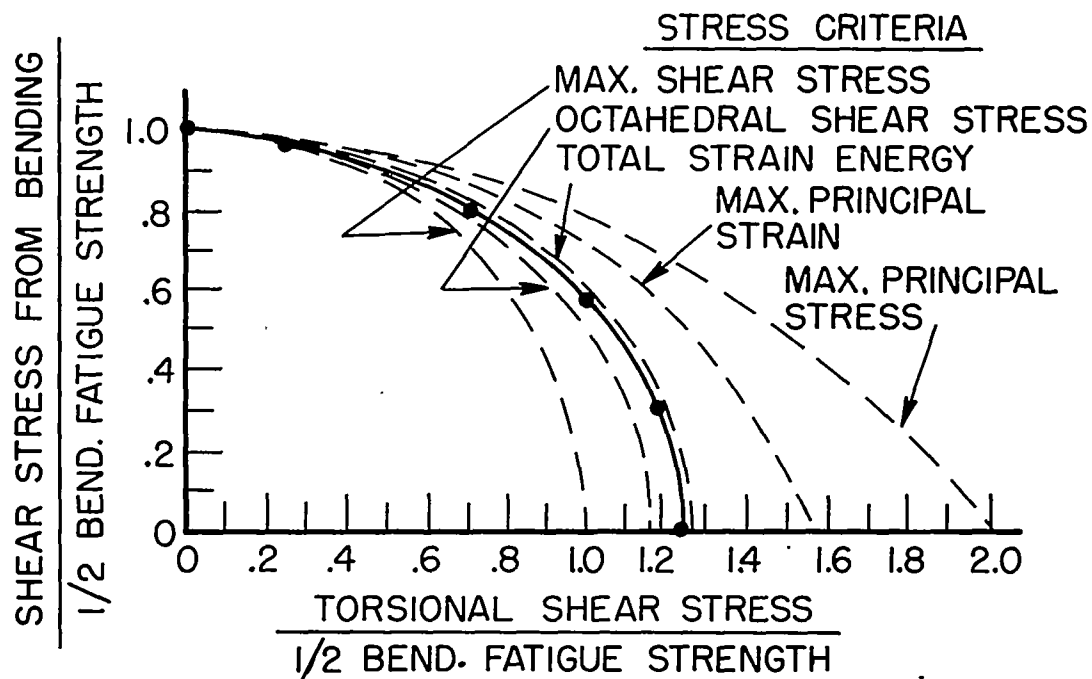
^bComposition: 0.45 carbon, 0.83 molybdenum, 0.016 phosphorus, 0.035 sulfur, and 0.19 silicon.

TABLE 3

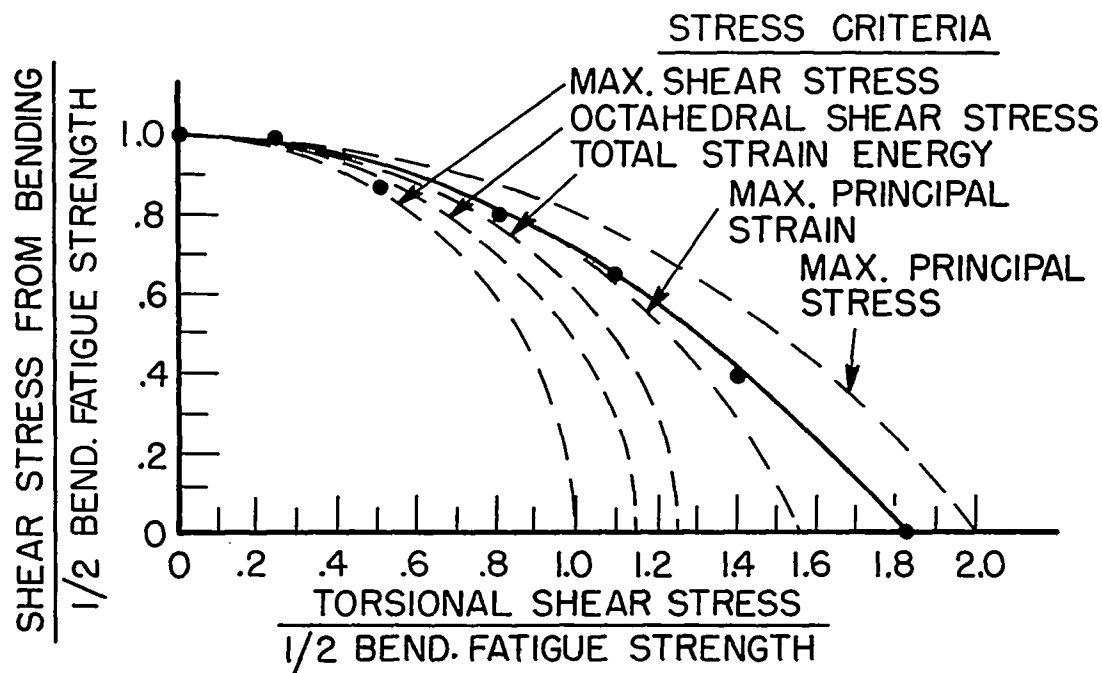
EFFECTS OF STRESSES ON CRACKS OF VARIOUS ORIENTATIONS

[N , applied normal component; S_s , applied shear component; σ_{\max} , maximum local normal stress; θ , position of maximum stress; τ_{\max} , maximum local shear stress]

	A					B					C				
															
Orientation	$N \times \sigma_1$	$S_s \times \sigma_1$	$\sigma_{\max} \times \sigma_1$	θ , deg	$\tau_{\max} \times \sigma_1$	$N \times \sigma_1$	$S_s \times \sigma_1$	$\sigma_{\max} \times \sigma_1$	θ , deg	$\tau_{\max} \times \sigma_1$	$N \times \sigma_1$	$S_s \times \sigma_1$	$\sigma_{\max} \times \sigma_1$	θ , deg	$\tau_{\max} \times \sigma_1$
1	1	0	11	0	5.5	1	0	11	0	5.5	1	0	11	0	5.5
2	.85	.35	11	20	5.5	.78	.53	11	24	5.5	.71	.71	13	24	6.5
3	.50	.50	9	24	4.5	.25	.75	9	30	4.5	0	1	11	45	5.5
4	.15	.35	4	40	2.0	.28	.53	7	40	3.5	-.71	.71	13	24	6.5
5	0	0	0		0	.50	0	5.5	45	2.8	-1	0	-11	0	5.5



(a) Chrome-vanadium steel.



(b) "Silal" cast iron.

Figure 1.- Interaction of bending and torsion in fatigue. (Data from ref. 1.)

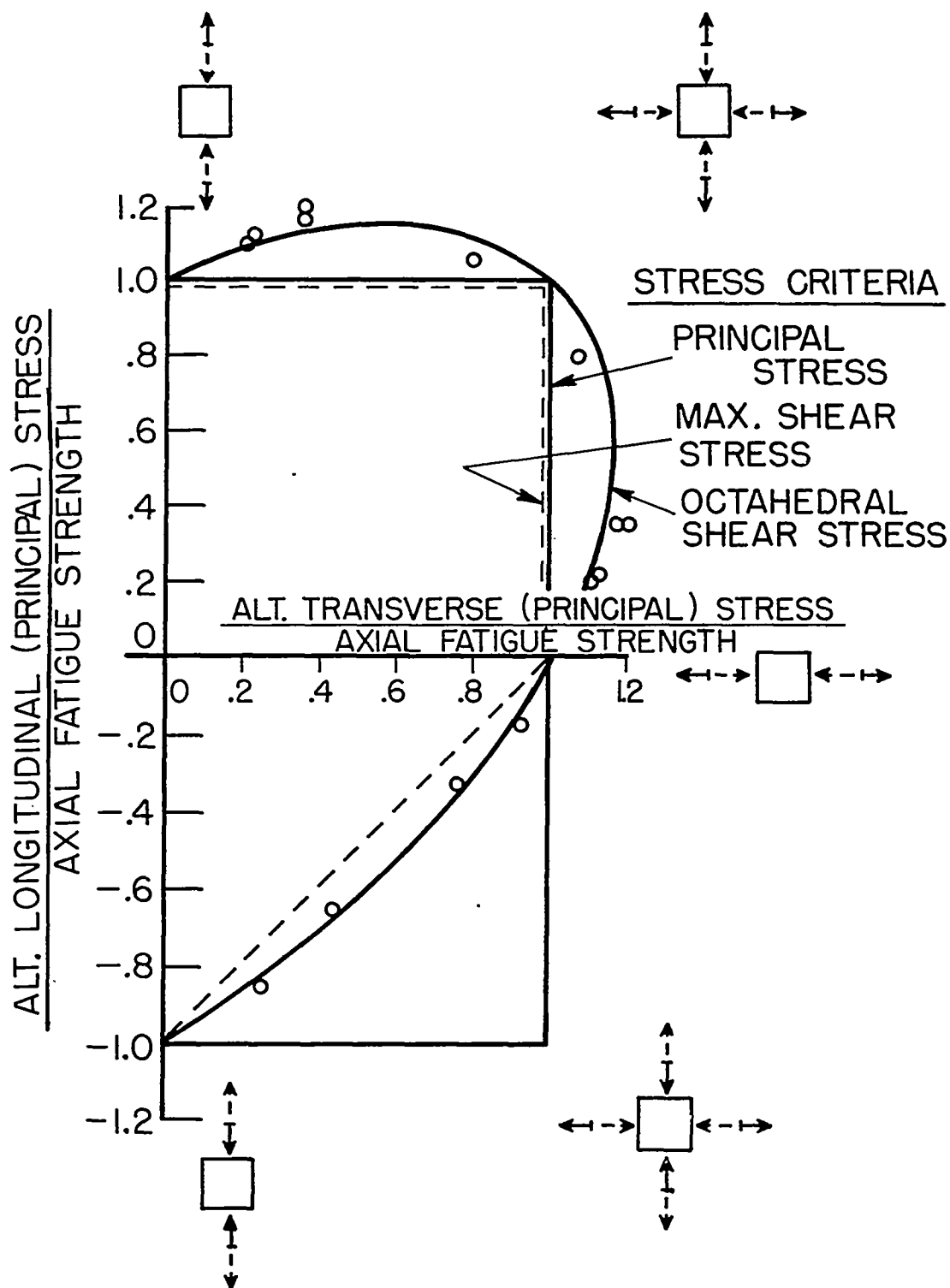


Figure 2.- Comparison of Sawert's data (ref. 4) with failure criteria.
 Annealed mild steel; fatigue strength at 10^7 cycles of reversed stress.

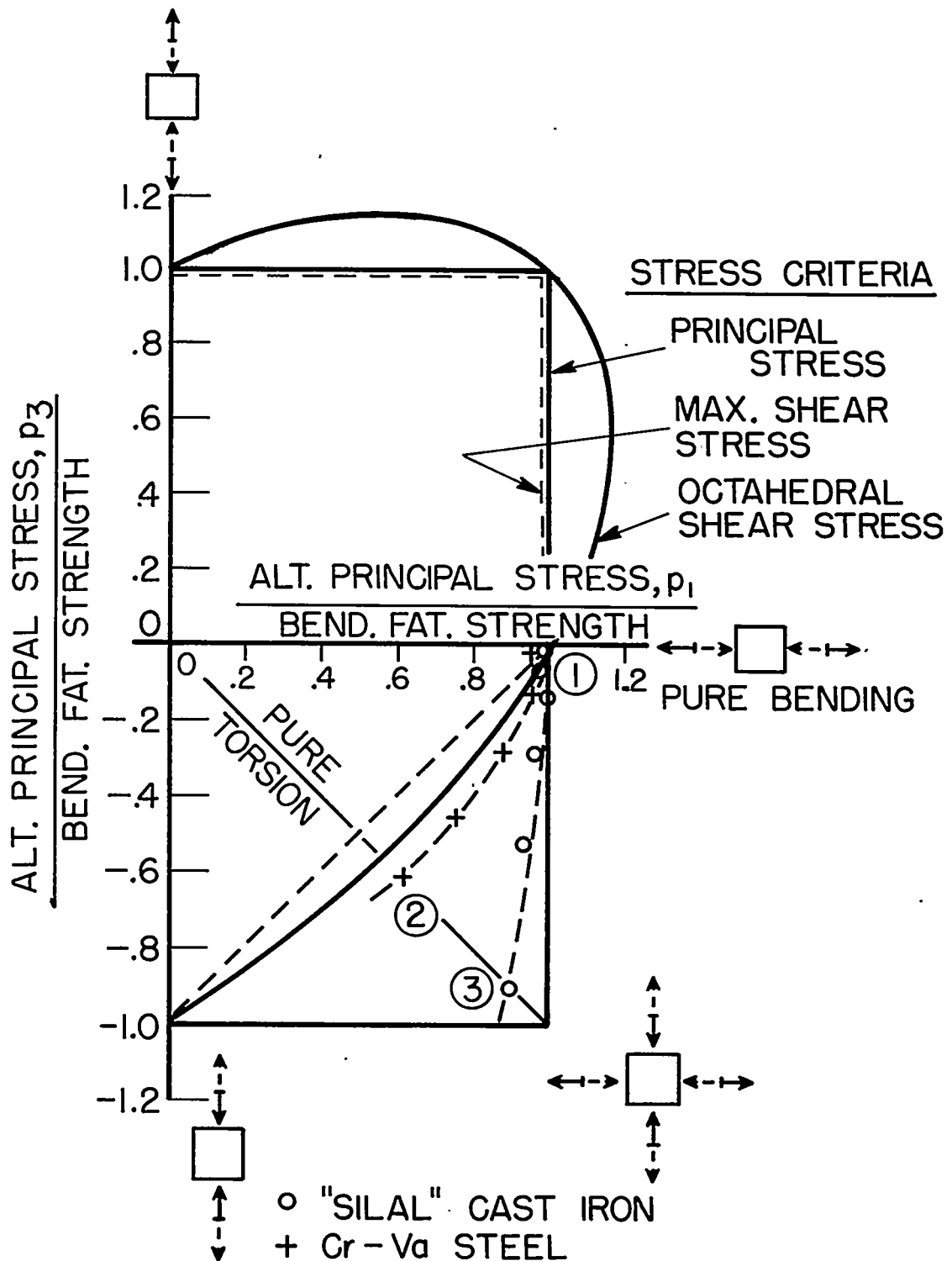


Figure 3.- Comparison of Gough's combined bending and torsion data (ref. 1) with failure criteria. Fatigue strength at 10^7 cycles of reversed stress.

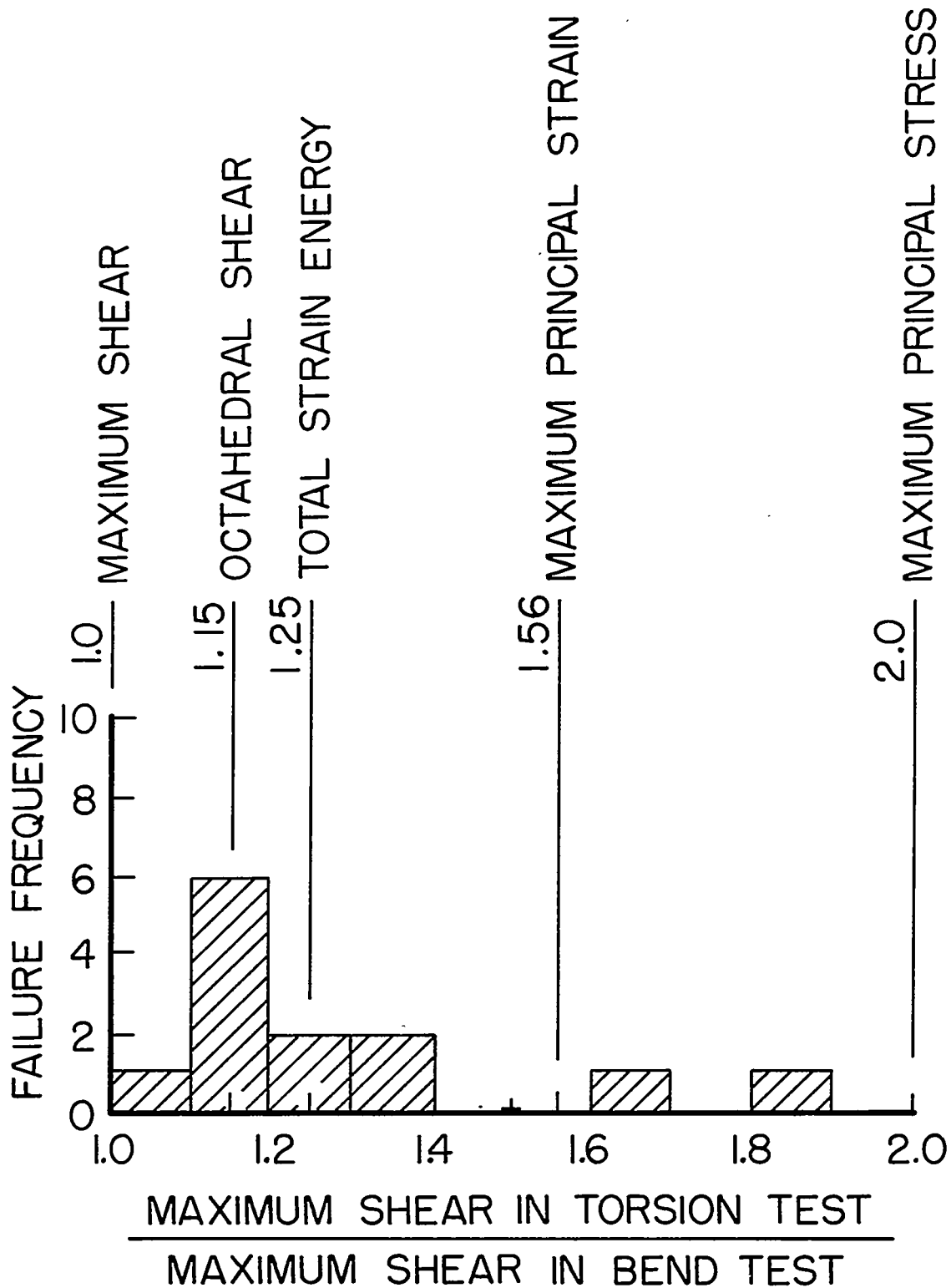
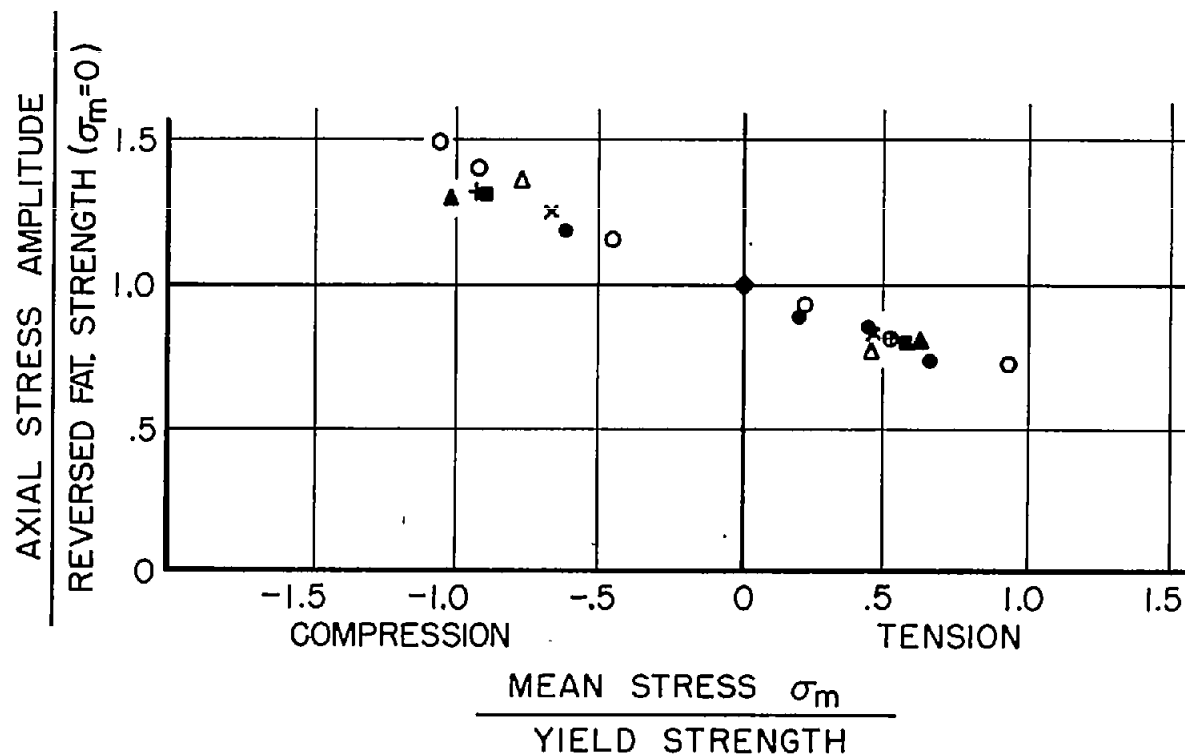


Figure 4.- Comparison of torsion and bending fatigue tests with failure criteria. (Data from ref. 1.)



MATERIAL	FATIGUE STRENGTH	YIELD	SOURCE
× 2024-T (24S-T) ALUM.	±26,000 psi	48,000 psi	NEWMARK AND COWORKERS (REF. 15)
○ 0.41 C STEEL	±36,000	55,000	NISHIHARA AND SAKURAI (REF. 13)
+ .65 C STEEL	±38,000	57,000	NISHIHARA AND SAKURAI (REF. 13)
△ .44 C STEEL	±33,000	57,000	NISHIHARA AND SAKURAI (REF. 13)
● DURALUMIN	±17,000	32,000	NISHIHARA AND KOJIMA (REF. 39)
■ MILD STEEL	±26,000	38,000	ROS AND EICHINGER (REF. 5)
▲ MILD STEEL	±37,000	47,000	ROS AND EICHINGER (REF. 5)

Figure 5.- Effect of mean axial stress on axial fatigue.

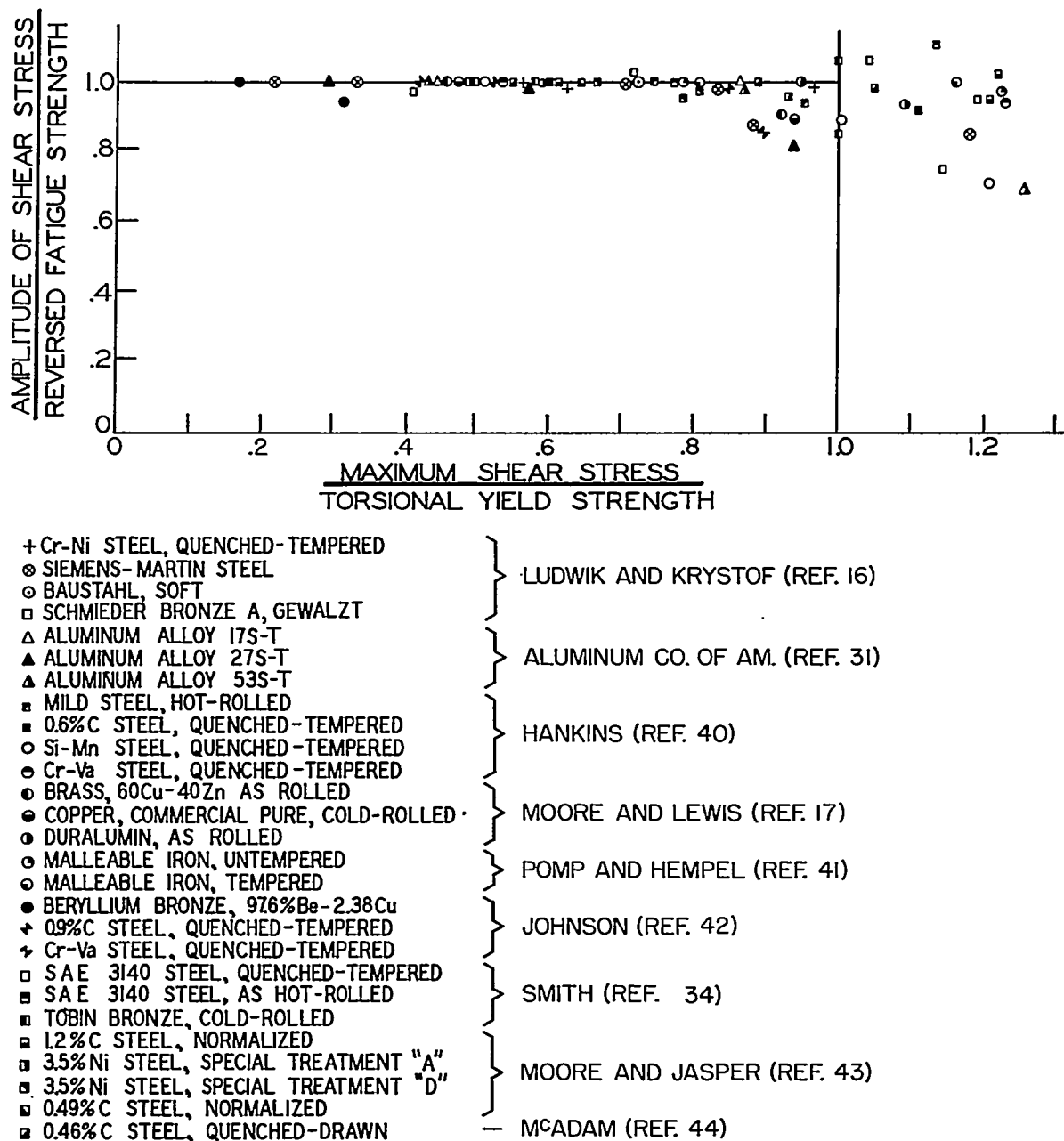
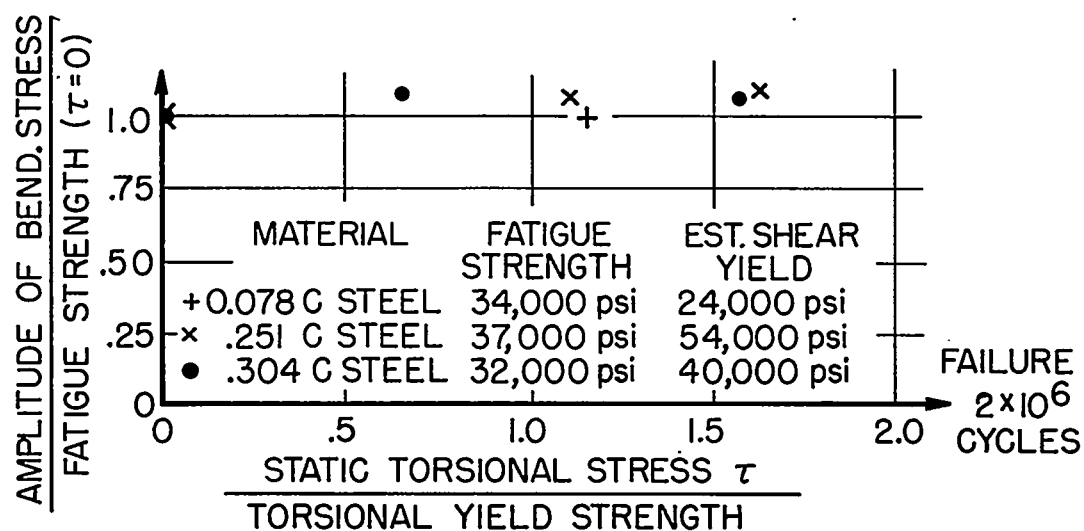
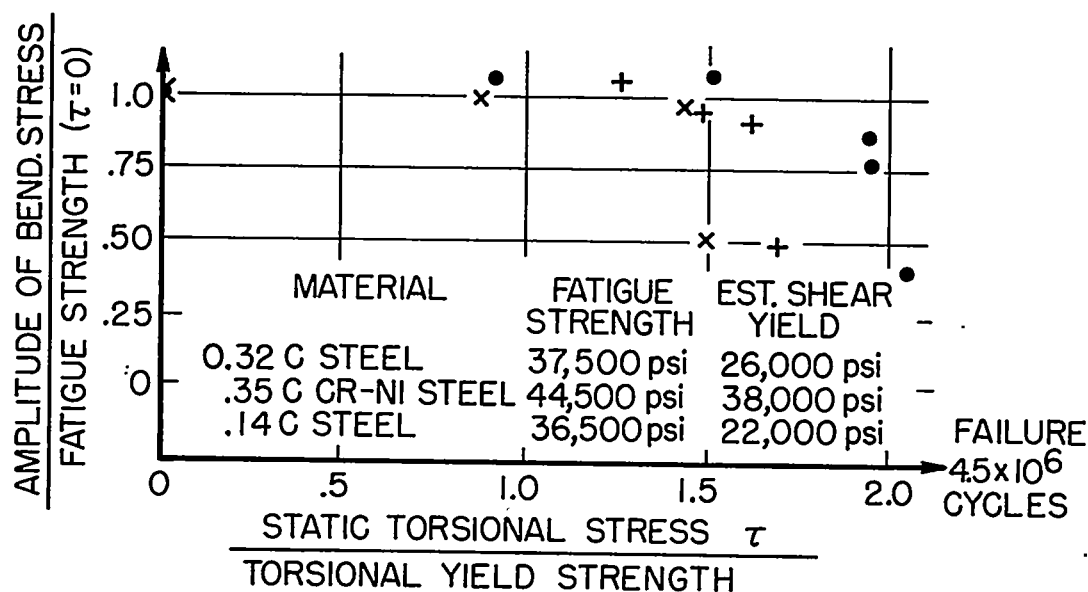


Figure 6.- Effect of static stress on range of shear stress. (Data from ref. 14.)

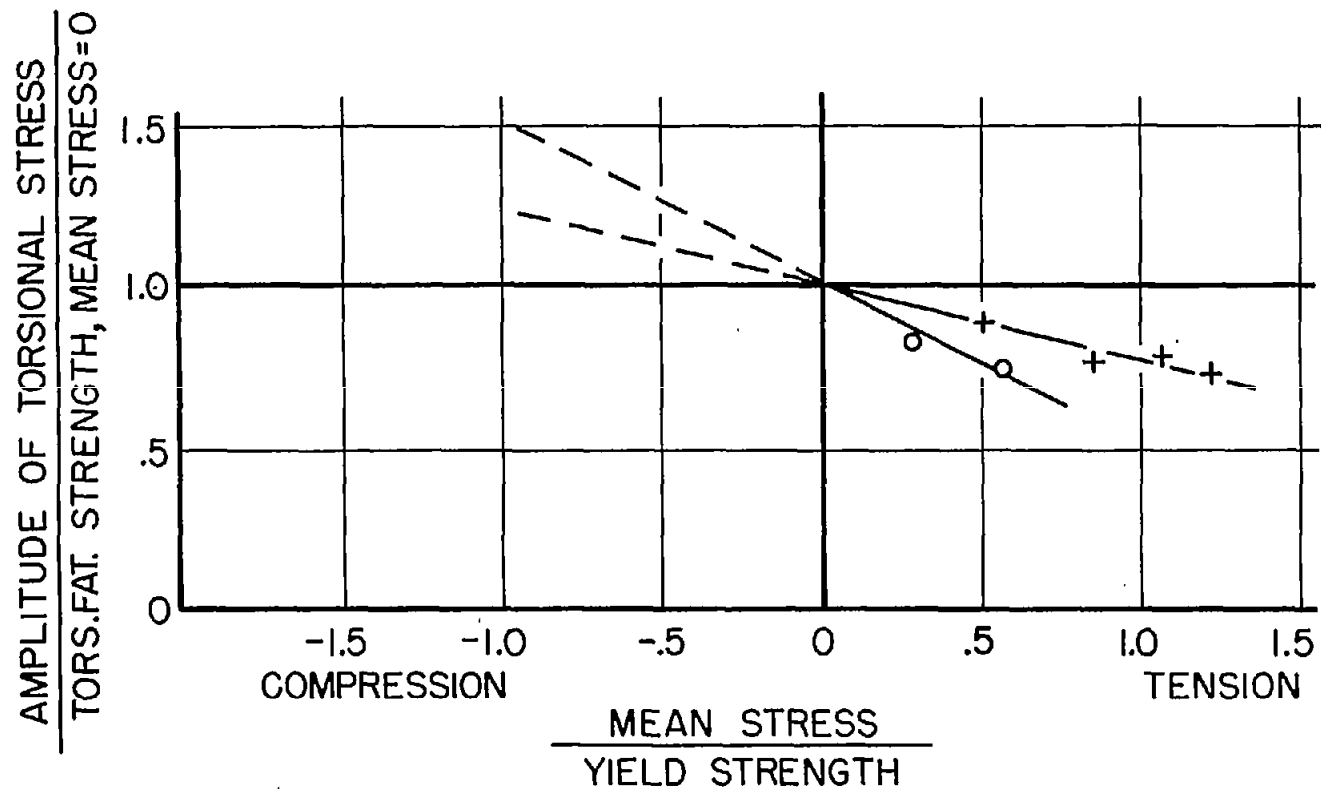


(a) Data from reference 20.



(b) Data from reference 19.

Figure 7.- Effect of static shear on permissible amplitude of alternating bending stress.



MATERIAL	MEAN STRESS	FATIGUE STRENGTH	YIELD	SOURCE
o Ni-Cr-Mo STEEL	BENDING	\pm 53,800 psi	137,000 psi	GOUGH (REF. 1)
+ MILD STEEL	AXIAL	\pm 16,400 psi	33,000 psi	HOHENEMSER & PRAGER (REF. 45)

Figure 8.- Effect of static normal stress on torsional fatigue.

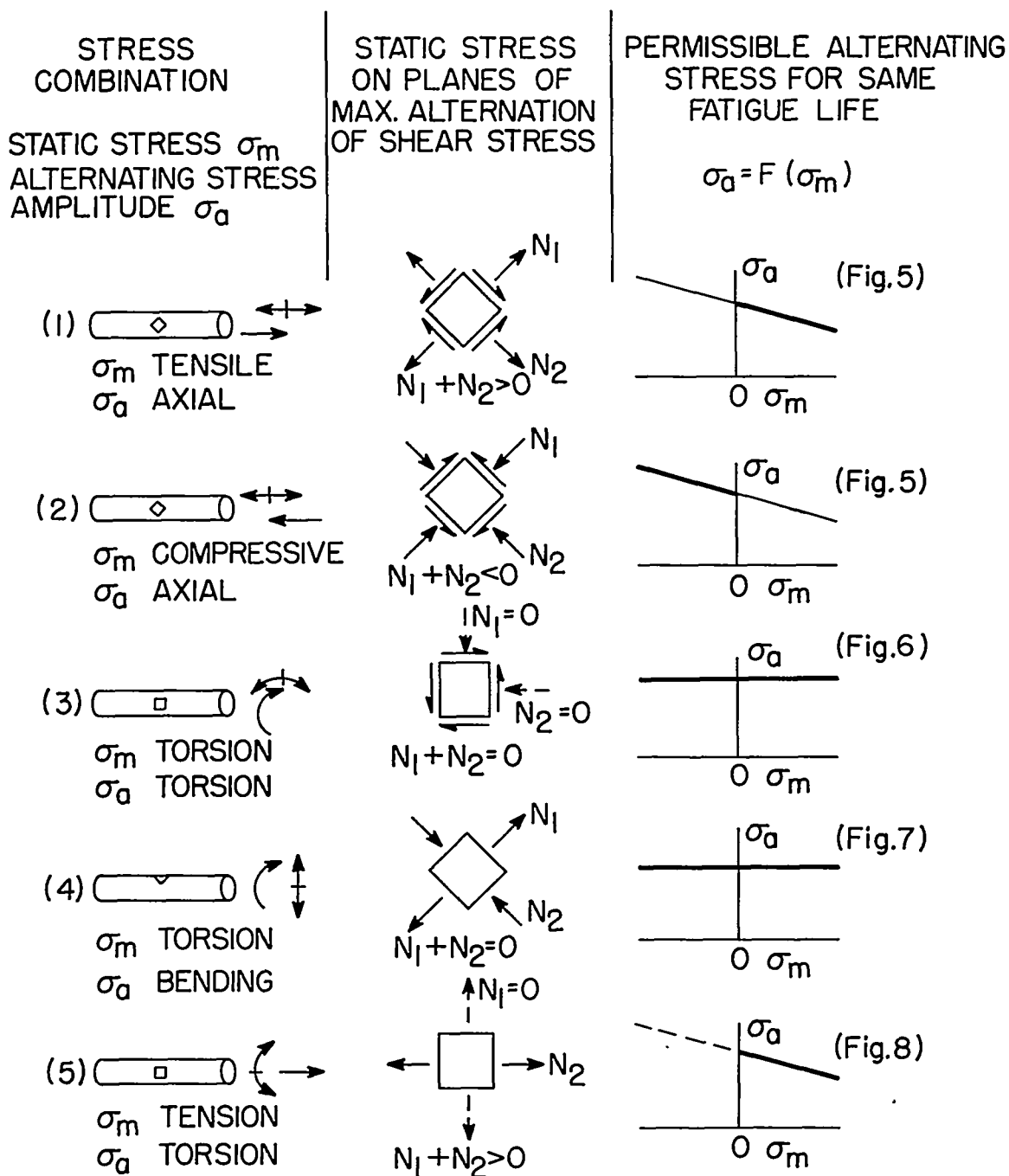


Figure 9.- Summary of effect of different combinations of static and alternating stresses on fatigue life.

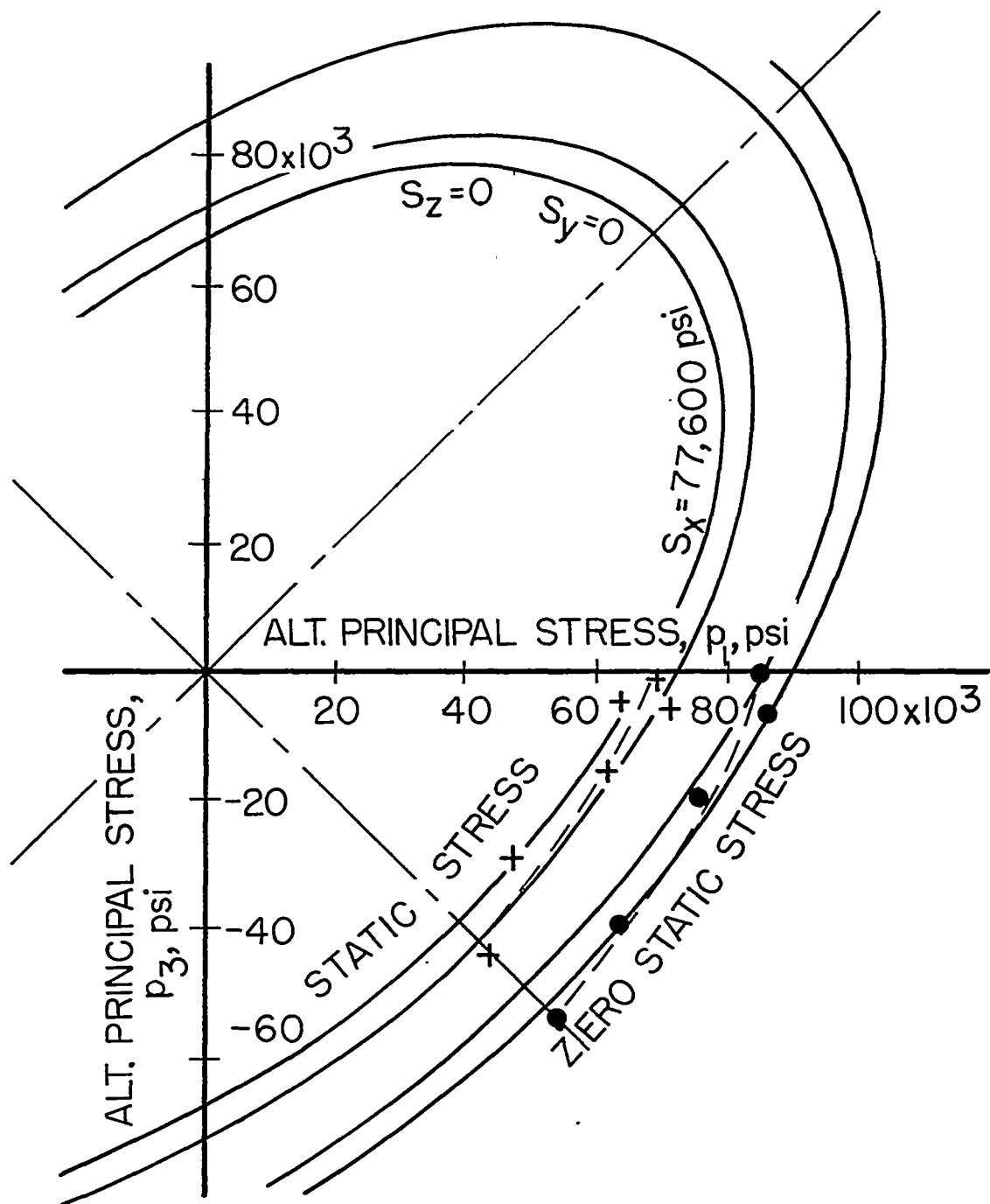
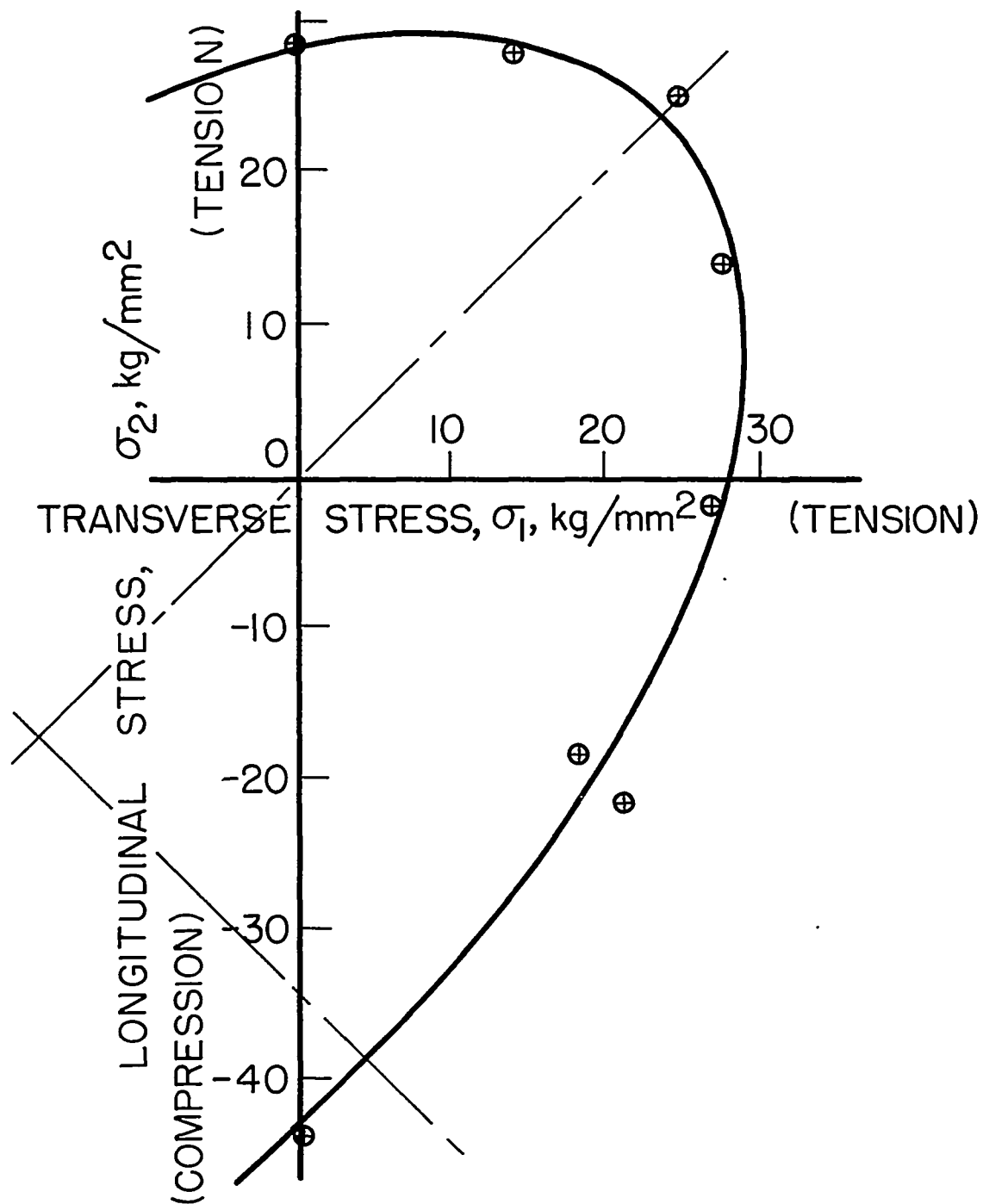


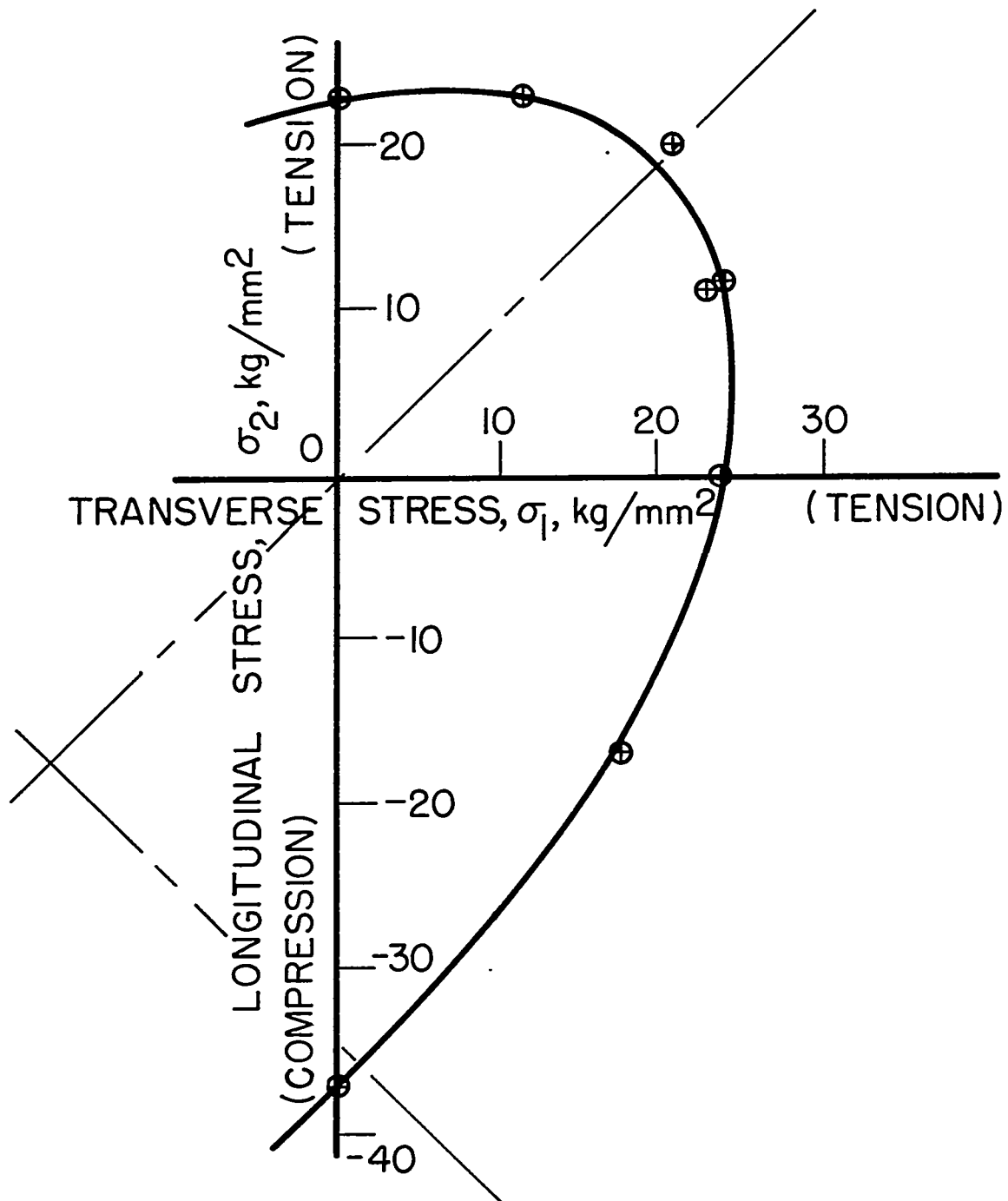
Figure 10.- Comparison of Gough's combined-stress fatigue data (ref. 1) with general stress criterion. Nickel-chromium-molybdenum steel; alternating stress; failure at 10^7 cycles. General criterion,

$$\frac{1}{3} \sqrt{(p_1 - p_2)^2 + (p_1 - p_3)^2 + (p_2 - p_3)^2} \leq A - \alpha (S_x + S_y + S_z).$$



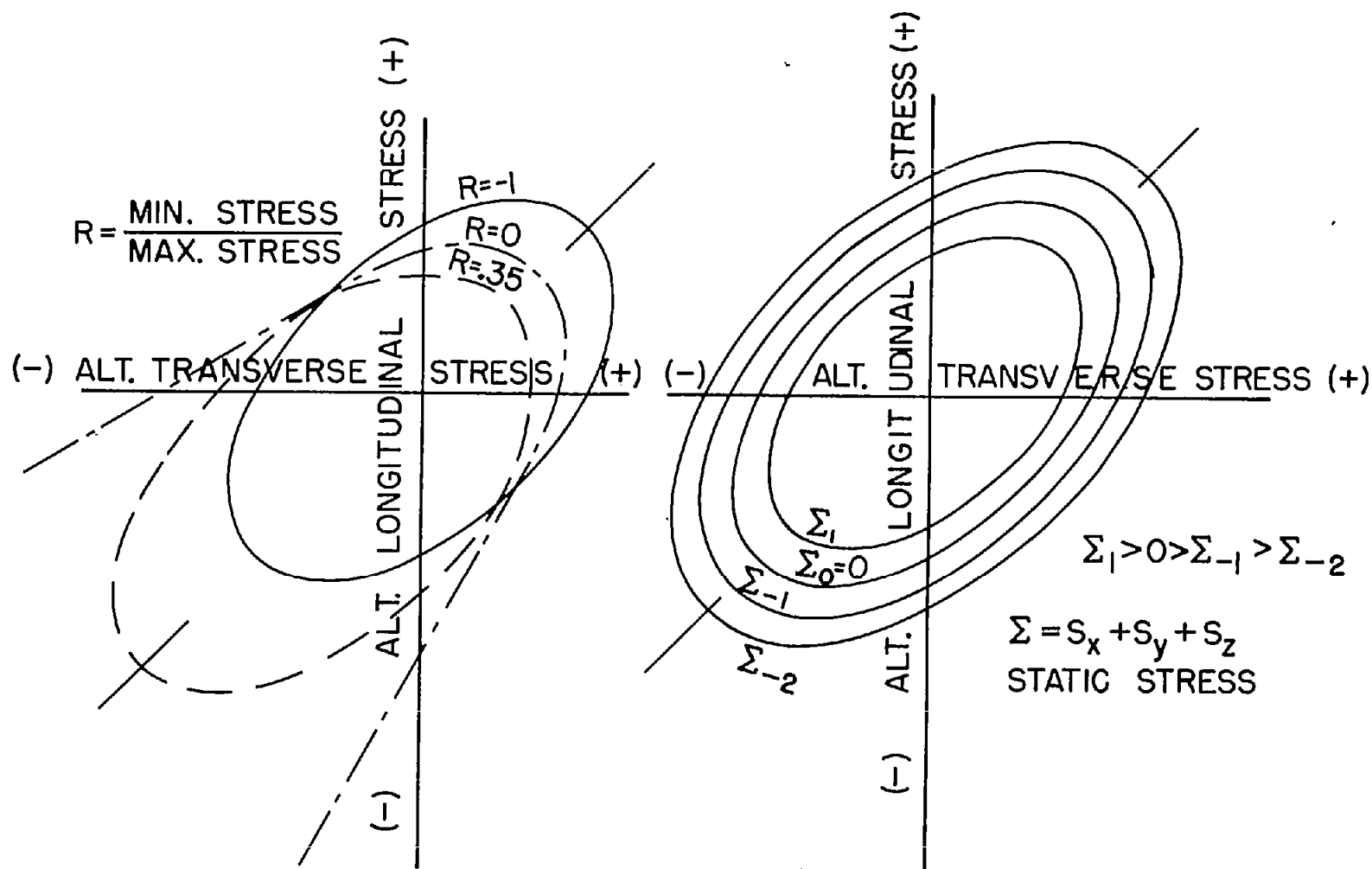
(a) Cast steel. Yield stress, 30 kg/mm²; failure at 10⁶ cycles.

Figure 11.- Comparison of Roß and Eichinger's combined-stress fatigue data (ref. 5) with general stress criterion transformed for fluctuating cycle. Minimum stress, 0.



(b) Aluminum alloy "Avional D." Yield stress, 33 kg/mm^2 ; failure at 10^6 cycles.

Figure 11.- Concluded



(a) Ratio of minimum to maximum stress.

(b) Sum of static stresses.

Figure 12.- Choice of parameters for combined-stress fatigue tests.

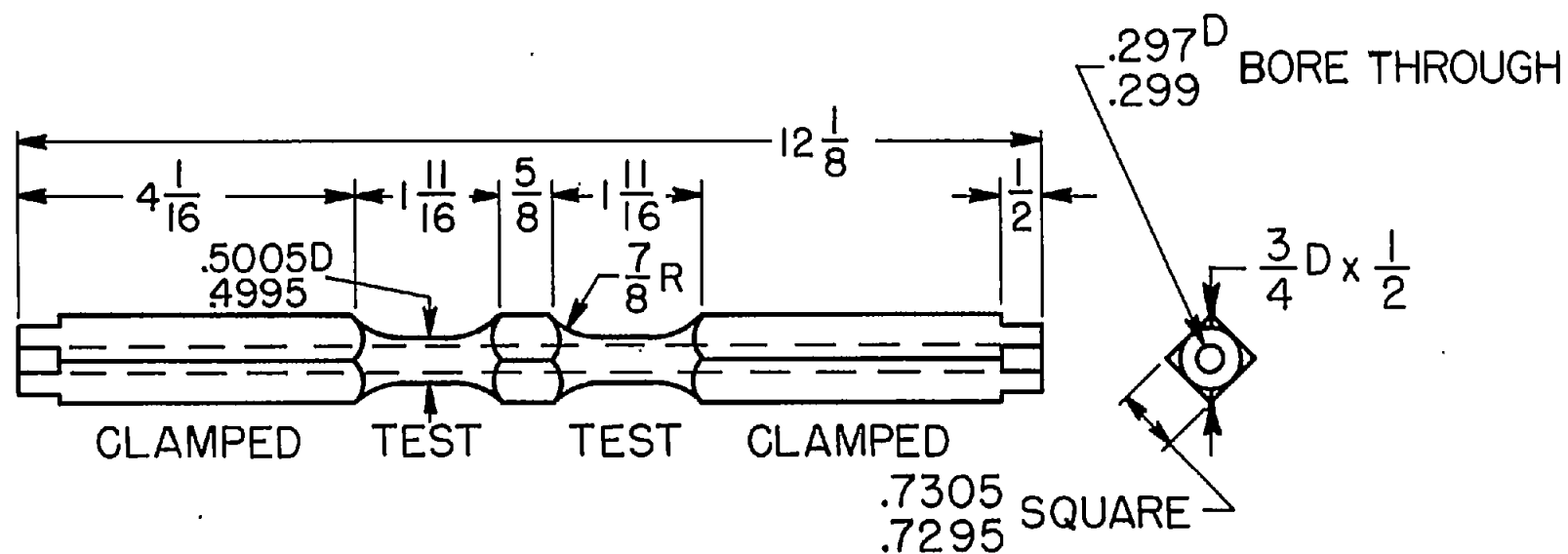
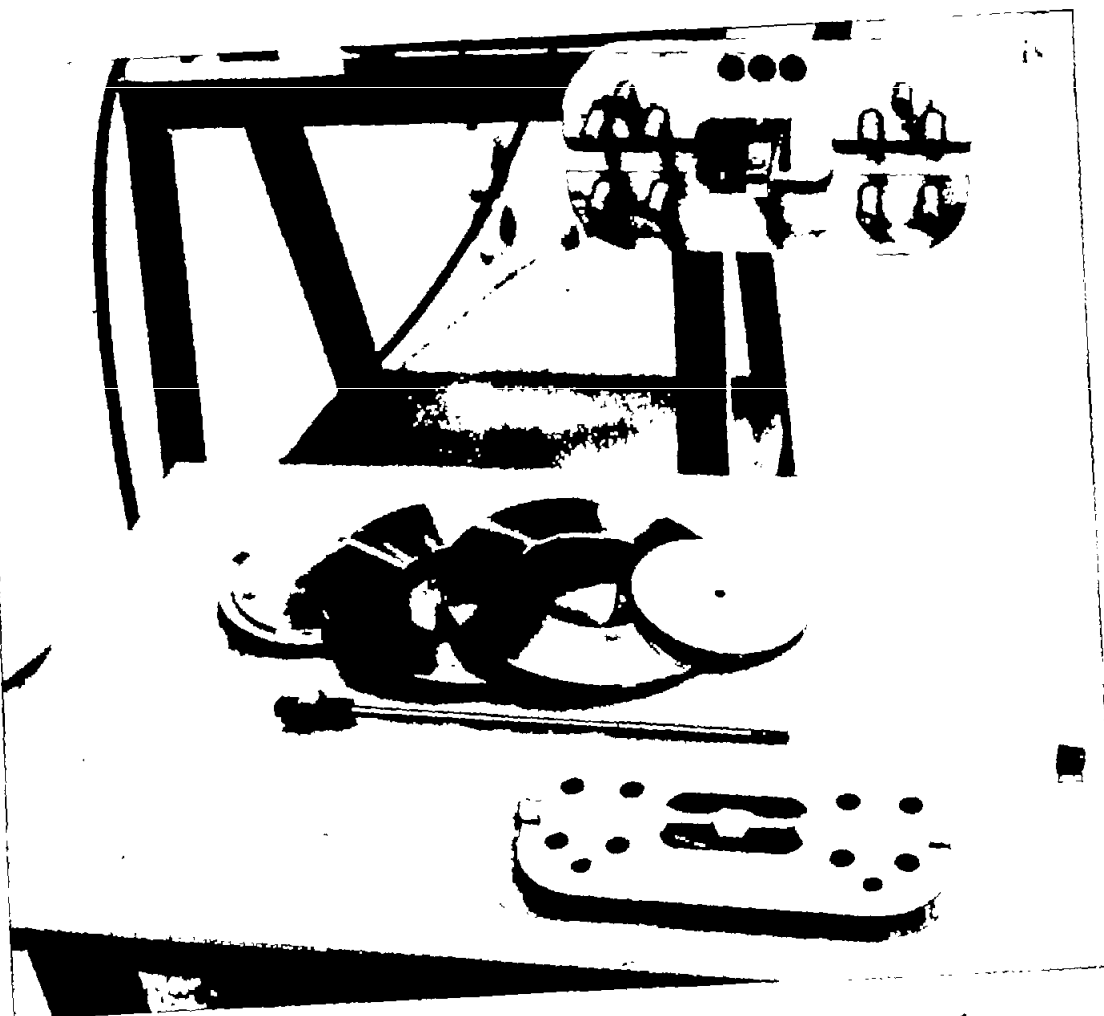


Figure 13.- Fatigue specimen. Alternating torsion; static compression.
Clamped surfaces true and in line ± 0.0005 ; ends faced smooth and square.



L-89367

Figure 14.- Disassembled prestressing device, fatigue specimen, and clamping frame.

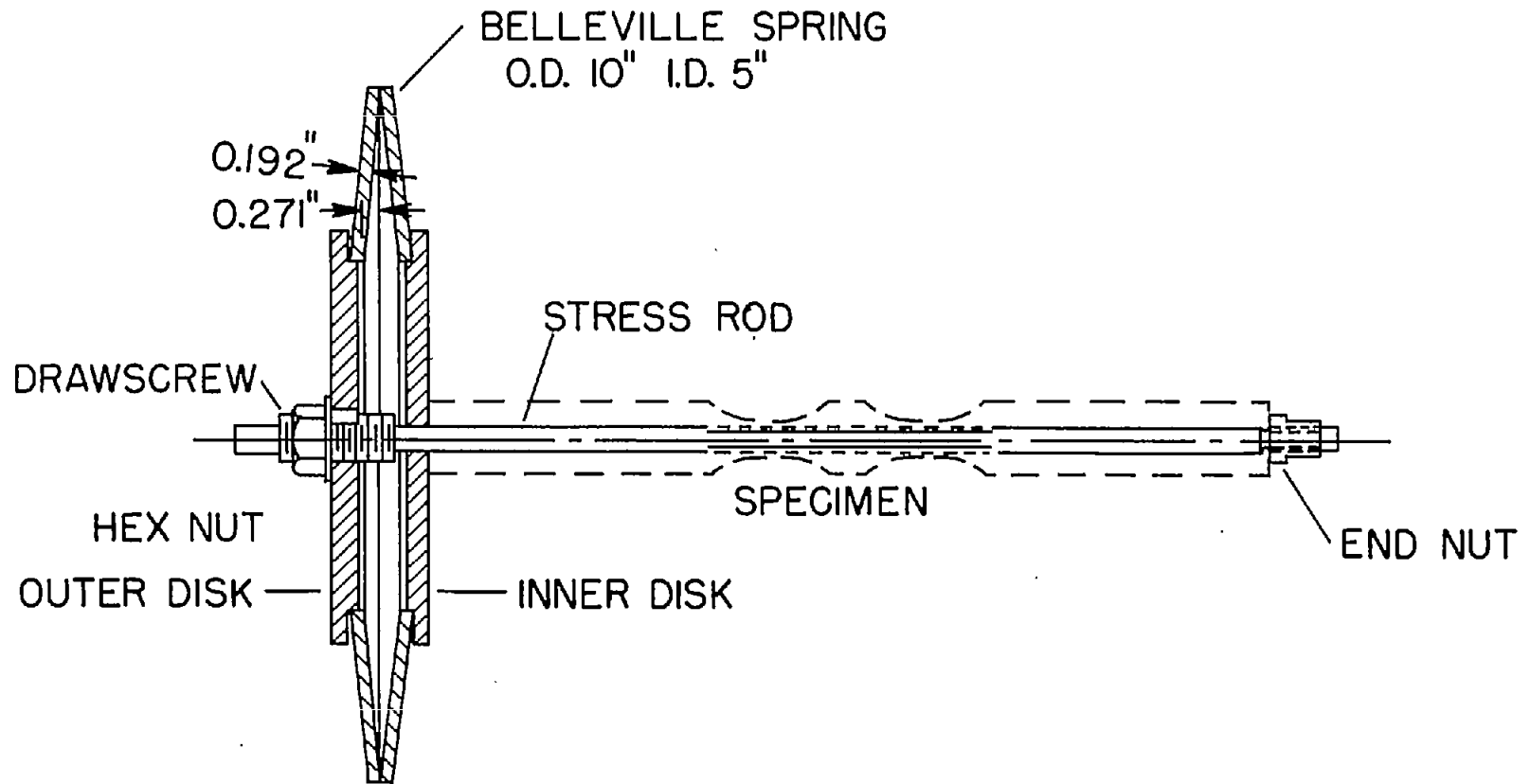


Figure 15.- Compressing device attached to specimen.

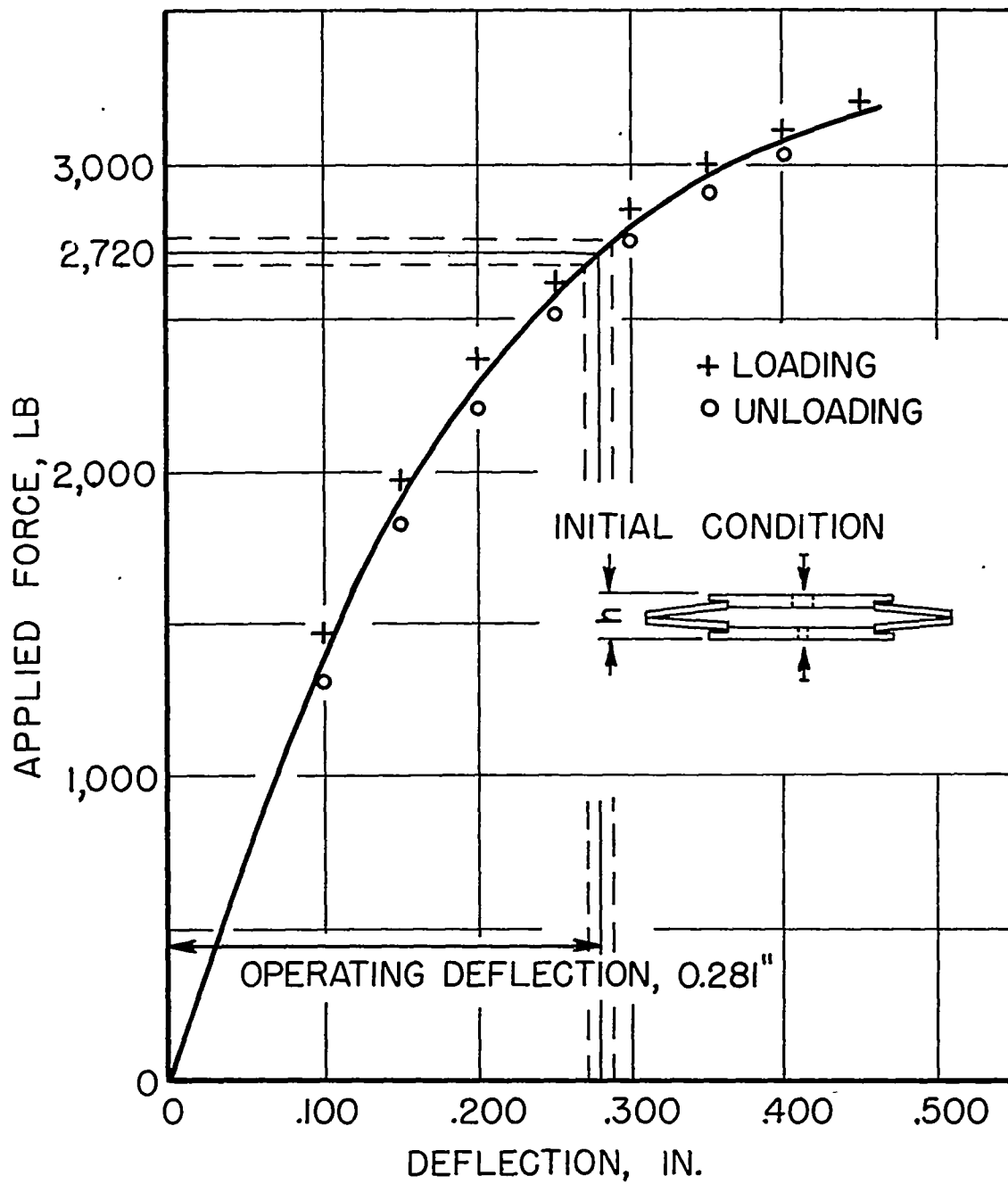
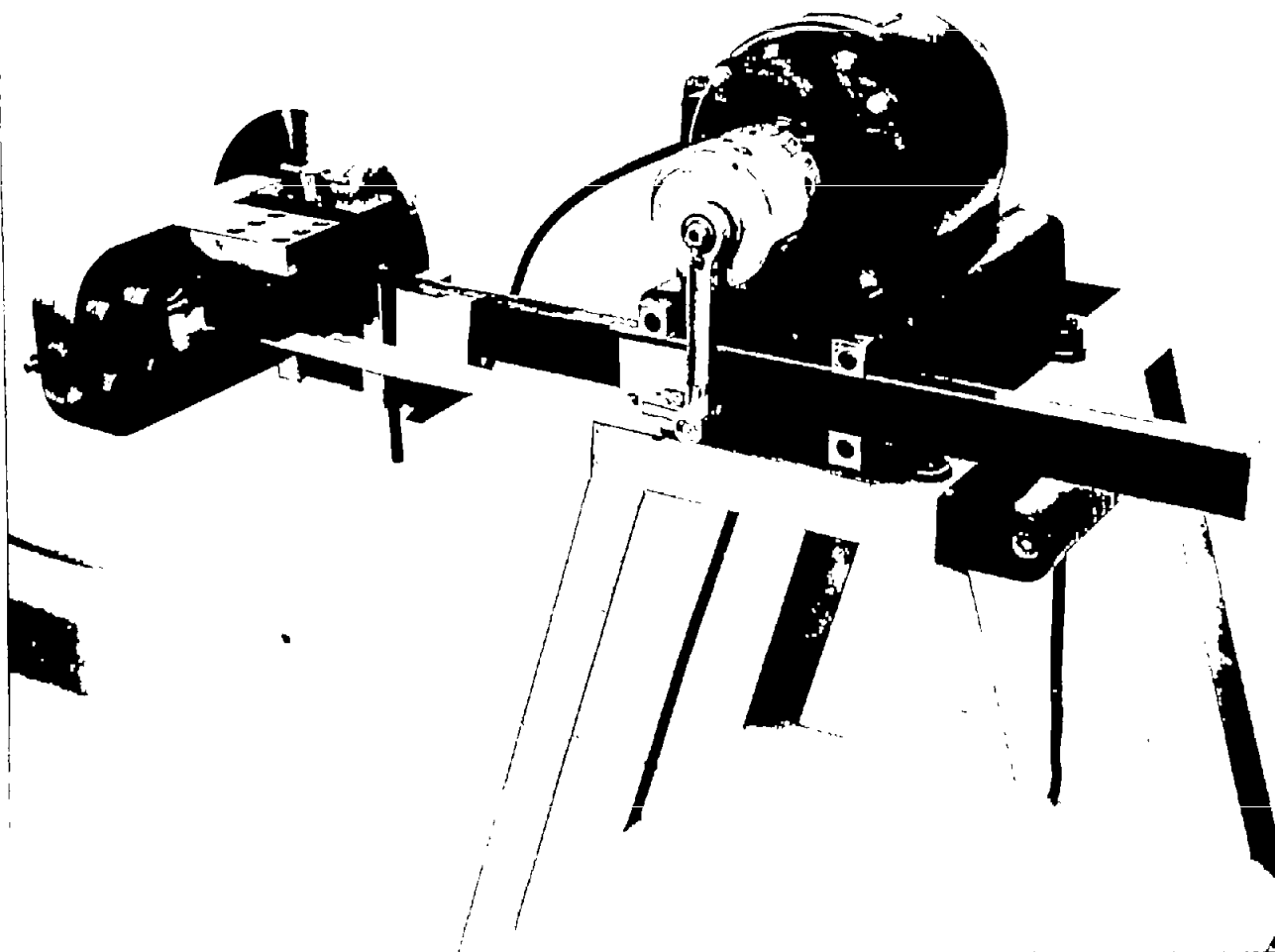


Figure 16.- Calibration of Belleville spring assembly. Load held for 5 minutes at each point; $h = 1.390$ inches for zero load.



L-89368
Figure 17.- Fatigue machine with torsion adaptation.

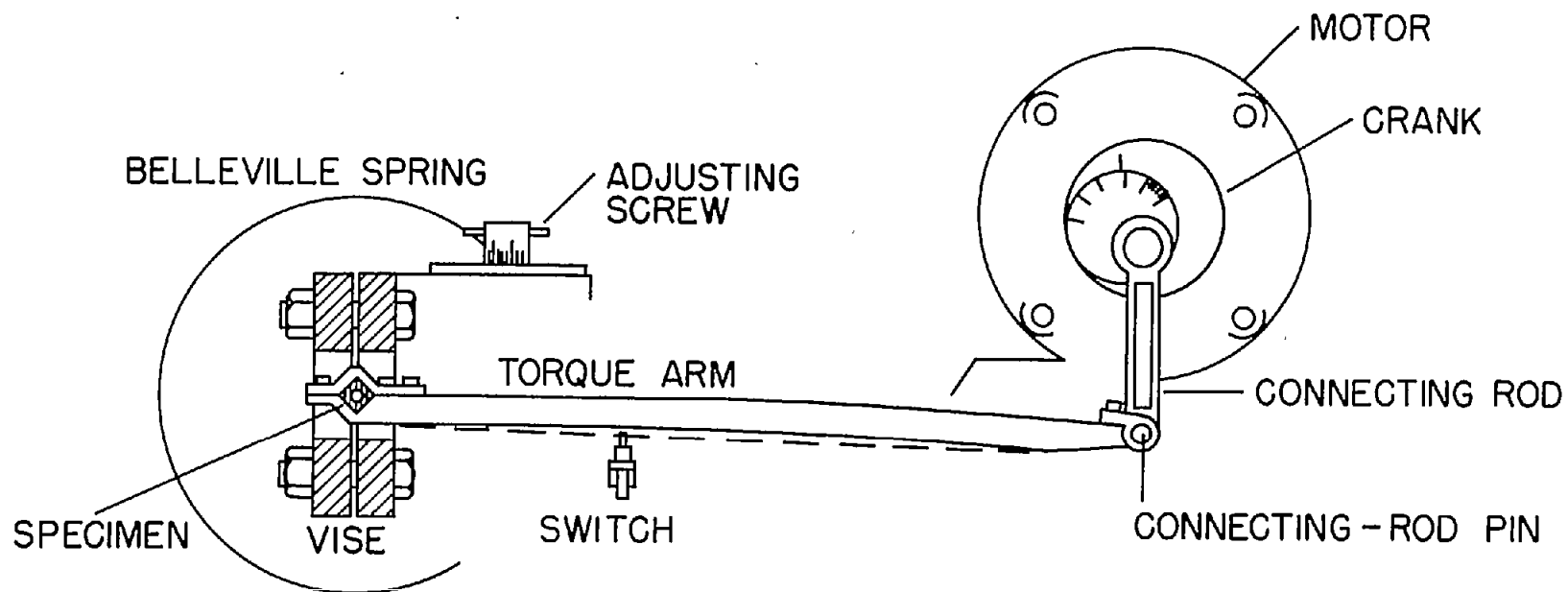


Figure 18.- Torsional fatigue testing mechanism.

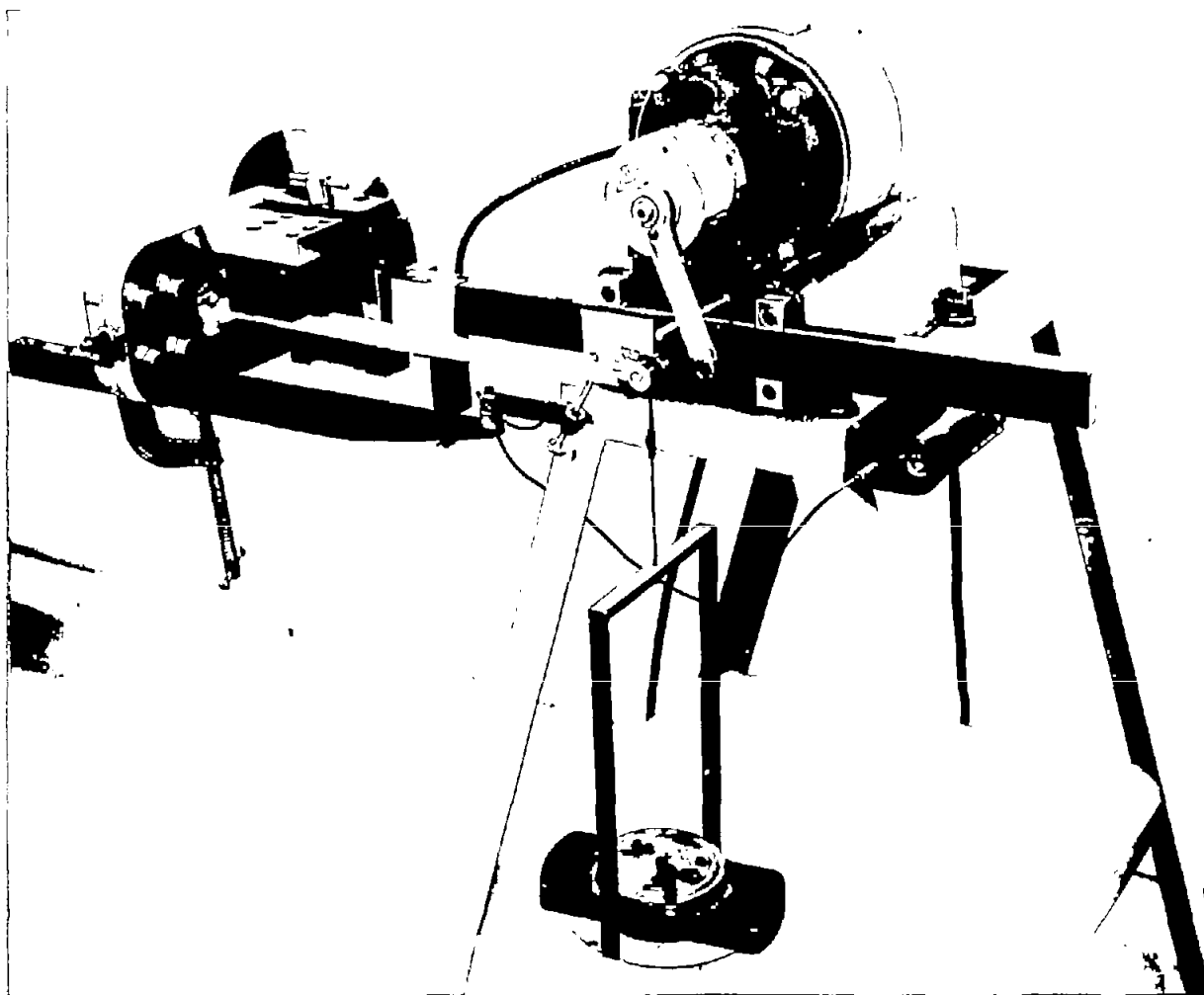


Figure 19.- Torsional fatigue tester with calibration weights and
deflection indicator. L-89369

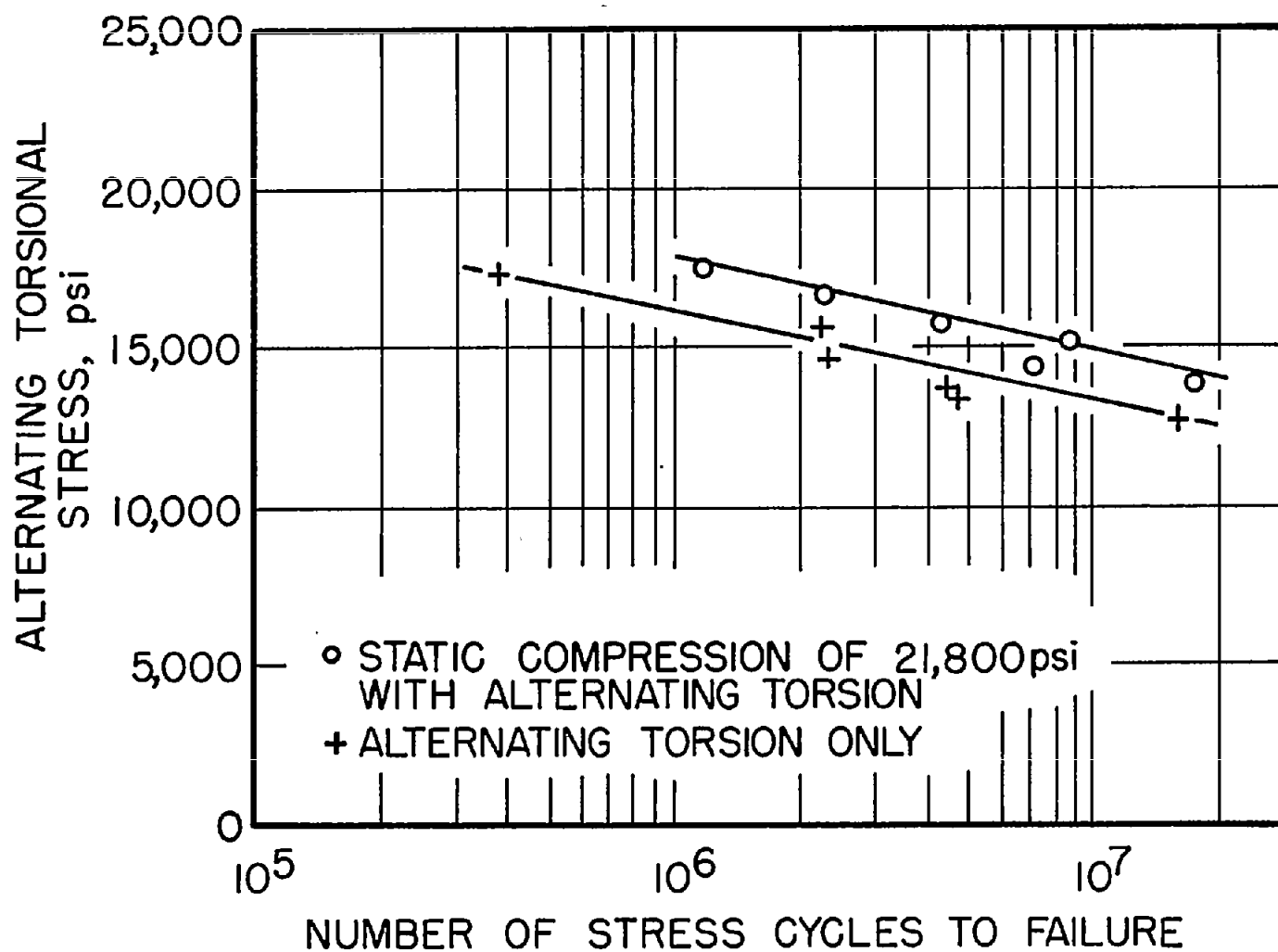
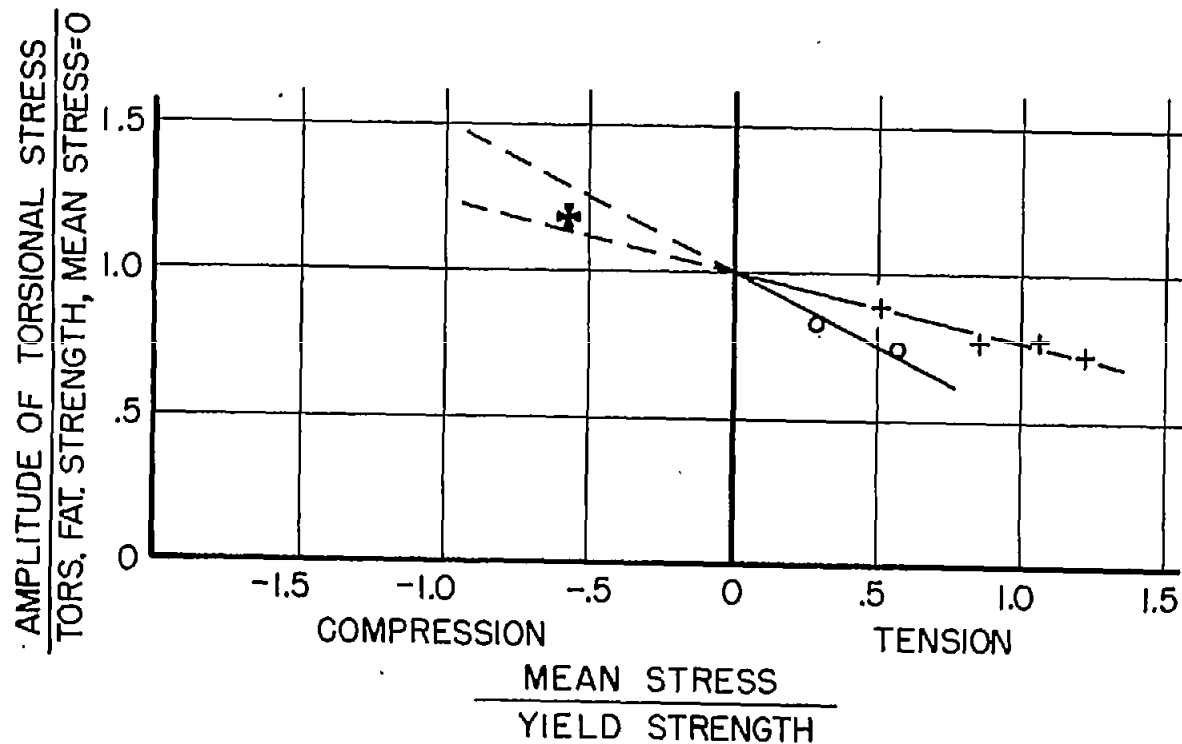
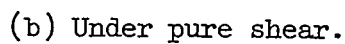
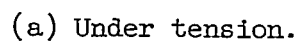


Figure 20.- Fatigue test results. Wrought aluminum alloy 6061-T6.



MATERIAL	MEAN STRESS	FATIGUE STRENGTH	YIELD	SOURCE
○ Ni-Cr-Mo STEEL	BENDING	$\pm 53,800$ psi	137,000 psi	GOUGH (REF. 1)
+ MILD STEEL	AXIAL	$\pm 16,400$ psi	33,000 psi	HOHENEMSER & PRAGER (REF. 45)
✚ 6061-T6 ALUM.	AXIAL	$\pm 13,000$ psi	40,000 psi	SINES (REF. 29)

Figure 21.- Effect of static normal stress on torsional fatigue.



NACA - Langley Field, Va.